A reconsideration of the lunar wake boundary based on Kaguya observations

*Masaki N Nishino[1], Yoshifumi Saito[2], Hideo Tsunakawa[3], Yuki Harada[4], Shoichiro Yokota[2], Futoshi Takahashi[5], Masaki Matsushima[3], Hidetoshi Shibuya[6], Hisayoshi Shimizu[7]

1. Institute for Space-Earth Environmental Research, Nagoya University, 2. ISAS/JAXA, 3. Tokyo Institute of Technology, 4. Space Science Laboratory, University of California, Berkeley, 5. Kyushu University, 6. Kumamoto University, 7. ERI, University of Tokyo

Refilling of the tenuous lunar wake by solar wind plasma has been one of the fundamental phenomena of planetary plasma sciences. Because a portion of the solar wind electrons has much higher speed than protons, it has been widely accepted that suprathermal electrons precede protons to come into the wake along the interplanetary magnetic field. In this model, ambipolar (inward) electric fields around the wake boundary generated by the charge separation attract the surrounding solar wind protons into the central lunar wake. However, such treatment has implicitly assumed one-dimensional motion of the solar wind plasma along the magnetic field perpendicular to the solar wind flow. Here we propose a new model of the wake boundary close to the Moon, based on Kaguya observations in orbit around the Moon; Solar wind protons come into the lunar wake owing to their gyro motion and large inertia without help of suprathermal electrons, and those protons form positively charged regions and outward electric fields around the wake boundary that should attract surrounding solar wind electrons. This new model well explains electron signatures around the wake boundary detected by Kaguya at ~100 km altitude from the lunar surface.

Keywords: Lunar wake, Solar wind, Electric field, Kaguya (SELENE)

Global mapping of the lunar magnetic anomalies by electron reflection method

*Daiba Kato[1], Yoshifumi Saito[2], Shoichiro Yokota[2], Masaki N Nishino[3], Hideo Tsunakawa[4]

1. Department of Earth and Planetary Science, The University of Tokyo, 2. Japan Earospace Exploration Agency Institute of Space and Astronautical Science, 3. Institute for Space-Earth Environmental Research, Nagoya University, 4. Deparment of Earth and Planetary Sciences, Tokyo Institute of Technology

Crustal magnetic fields are known to exist on Earth, Mars, and the Moon, and they may also exist on various astronomical bodies in the Solar System. Although the Moon has no global magnetic field, there exist locally magnetized regions called lunar magnetic anomalies. Therefore incident solar wind directly impacts the lunar surface, except for the case where the crustal magnetic field prevents it from penetrating into the lunar magnetic anomalies. Interaction between the lunar magnetic anomalies and plasma particles give important information about the distribution of plasma environment and space weathering. Electron reflection measurement is one of the methods for observing the lunar magnetic anomalies. This measurement makes use of the magnetic mirror effect. By the existence of the lunar magnetic anomalies, if the pitch angle of an incident electron reaches 90 degrees before the electron impacts the lunar surface, it is reflected back to the satellite. The crustal magnetic fields on the lunar surface can be estimated by measuring the cutoff pitch angle of the reflected electrons and the magnetic field around the satellite. This method can infer the lunar surface field strength with sensitivity that is independent of spacecraft altitude.
Apollo revealed hundreds of localized crustal magnetic fields. Lunar Prospector made a global map of the crustal magnetic fields for the first time. Kaguya observed the more detailed global crustal magnetic fields with higher time resolution and higher spatial resolution than the previous observations.
We have analyzed the reflected electron data and magnetic field data around the satellite obtained by low energy charged particle analyzers (MAP-PACE) and magnetometer (MAP-LMAG) on Kaguya. Using the electron reflection method, we will report the global map of the lunar surface magnetic fields with high spatial resolution (~8 km). Some of the observations of the reflected electron distributions showed energy-dependent loss cone by the effects of electrical potential differences between the lunar surface and Kaguya. We corrected the influence of the electrical potential difference on our result. By comparing our result of electron reflection method with the magnetic field measured by the magnetometer, we will discuss the behavior of the electron reflection over the lunar surface.

Keywords: Moon, Magnetic anomaly, Kaguya, Electron reflection method

Secondary ions of carbon, nitrogen and oxygen from the Moon

*Shoichiro Yokota[1], Yoshifumi Saito[1], Kazushi Asamura[1], Masaki N Nishino[2], Hideo Tsunakawa[3]

1. Japan Earospace Exploration Agency Institute of Space and Astronautical Science, 2. Institute for Space-Earth Environmental Research, Nagoya University, 3. Tokyo Institute of Technology

Since the Moon has no global intrinsic magnetic field and only has a very thin atmosphere, the solar wind continuously bombard the lunar surface except when the Moon stays in the Earth's magnetosphere. The solar wind ion hitting causes the secondary ion emission from the lunar surface.
Although the initial energies of such secondary ions are low around several electron volts, the solar wind electric and magnetic fields pick up the ions and sometimes transport them to the outer space.
MAP(Magnetic field and Plasma experiment)-PACE(Plasma energy Angle and Composition experiment) on the Kaguya spacecraft performed the first direct ion measurements of three-dimensional energy and mass information. KAGUYA is a Japanese lunar orbiter which had conducted 1.5-year observation around an altitude of 100 km in 2008-2009. MAP consists of LMAG (Lunar MAGnetometer) and PACE. MAP-LMAG is a triaxial flux gate magnetometer which measures the vector magnetic field with a sampling frequency of 32 Hz and a resolution of 0.1 nT. MAP-PACE consists of four sensors: two electron sensors and two ion sensors. The two ion sensors are the IMA and the IEA. The IMA, the IEA and the two electron sensors have hemispherical FOVs and cover the full three-dimensional phase space of low-energy ions and electrons. Because Kaguya is a three-axis stabilized satellite, the IMA continuously faces the Moon. Thus, it measures ions that mostly come from the Moon, whereas the mounted IEA on the opposite side of the spacecraft measures ions from outer space. The nadir-pointing IMA measured ions which originated from the lunar surface and were at least composed of He+, C+, O+, Na+, K+ and Ar+. The measurements of ions from the Moon provided us with abundance mapping of the lunar secondary ions by the solar wind. We report the features of the lunar secondary ion abundance, especially of C+, N+ and O+ because such light species are well distinguished. We also discuss the feasibility of the remote observation of small bodies' surface materials by measuring secondary ions by the solar wind.

Keywords: Moon, Secondary ions, Mass analyses

KAGUYA observation of terrestrial oxygen transported to the Moon

*Kentaro Terada[1], Shoichiro Yokota[2], Yoshifumi Saito[2], Naritoshi Kitamura[2], Kazushi Asamura[2], Masaki N Nishino[3]

1. Department of Earth and Space Science, Graduate School of Science, Osaka University, 2. Institute of Space and Astronautical Science, Japan Aerospace Exploration Agency, 3. Institute for Space-Earth Environmental Research, Nagoya University

Oxygen, the most abundant element of Earth and Moon, is a key element to understand the various processes in the Solar system, since it behaves not only as gaseous phase but also as the solid phase (silicates). Here, we report observations from the Japanese spacecraft Kaguya of significant 1-10 keV O^+ ions only when the Moon was in the Earth’ s plasma sheet. Considering the valence and energy of observed ions, we conclude that terrestrial oxygen has been transported to the Moon from the Earth’ s upper atmosphere (at least 2.6×10^4 ions cm^{-2} sec^{-1}). This new finding could be a clue to understand the complicated fractionation of oxygen isotopic composition of the very surface of lunar regolith (particularly the provenance of a ^{16}O-poor component), which has been a big issue in the Earth and Planetary science.

Keywords: The Earth-Moon system , KAGUYA (SELENE), Oxygen, Magnetosphere, Solar Wind, Earth Wind

10-year summary of the studies based on global subsurface radar sounding of the Moon by SELENE (Kaguya) Lunar Radar Sounder (LRS)

*Atsushi Kumamoto[1], Yasushi Yamaguchi[2], Atsushi Yamaji[3], Takao Kobayashi[4], Shoko Oshigami[5], Ken Ishiyama[6], Norihiro Nakamura[7], Yoshitaka Goto[8], Junichi Haruyama[6]

1. Department of Geophysics, Graduate School of Science, Tohoku University, 2. Department of Earth and Environmental Sciences, Graduate School of Environment Studies, Nagoya University, 3. Division of Earth and Planetary Sciences, Graduate School of Science, Kyoto University, 4. Korea Institute of Geoscience and Mineral Resources, 5. Kogakuin University, 6. Institute of Space and Astronautical Science, Japan Aerospace Exploration Agency, 7. Institute for Excellence in Higher Education, 8. School of Electrical and Computer Engineering, Kanazawa University

The Lunar Radar Sounder (LRS) onboard the SELENE (Kaguya) spacecraft successfully performed subsurface radar sounding of the Moon and passive observations of natural radio and plasma waves from the lunar orbit. The operation of LRS started on October 29, 2007. Until the end of the operation on June 10, 2009, 2363 hours worth of radar sounder data and 8961 hours worth of natural radio and plasma wave data were obtained [Ono et al., 2010]. We found subsurface regolith layers at depths of several hundred meters, which were interbedded between lava flow layers in the nearside maria. [Ono et al., 2009]. Using the measured depths and structures of the buried regolith layers, we could determine several key parameters on tectonics, surface layer evolution, and volcanism in the maria: Base on the determined parameters such as the formation age of the ridges, effective permittivity of the uppermost basalt layers, and the lava flow volumes in the nearside maria, we made the following suggestions: (1) Global cooling, which forms ridges in southern Serenitatis, became dominant after 2.84 Ga. [Ono et al., 2009], (2) The porosity of the uppermost basalt layer in Mare Humorum was estimated to be 19-51%, much more than the average of Apollo rock samples (7%) [Ishiyama et al., 2013], and (3) The average eruption rate of the lava flow in the nearside maria was 10^{-3} km^{-3}/yr. at 3.8 Ga and decrease to 10^{-4} km^{-3}/yr at 3.3 Ga [Oshigami et al., 2014]. Thanks to the high downlink rate from the SELENE/LRS (0.5 Mbps), we could obtain almost raw (simply pulsecompressed) waveform data from the lunar subsurface radar sounding. Using this dataset, synthetic aperture radar (SAR) processing was applied with trying several permittivity models in the analyses on the ground [Kobayashi et al., 2012]. This dataset is provided via SELENE Data Archive (http://l2db.selene.darts.isas.jaxa.jp/index.html.en). Even after the SELENE operation ended, subsurface explorations of the Moon were carried on by several missions such as GLAIL and Chang'E-3. Detailed comparisons among subsurface datasets with different scale and different coverage will be important in future studies.

Keywords: SELENE, LRS, Lunar volcanic activity

Detection of the Lava Tubes by SELENE(Kaguya) Lunar Radar Sounder

*Tetsuya Kaku[1], Junichi Haruyama[2], Wataru Miyake[3], Atsushi Kumamoto[4], Ken Ishiyama[2], Takahiro Iwata[2], Sarah Crites[2]

1. Department of Aeronautics and Aerospace School of Engineering, Tokai University, 2. JAXA/ISAS, 3. Toaki University, 4. Department of Geophysics, Gradute School of Science, Tohoku University

Intact lava tubes on the Moon are potentially the best candidates for constructing lunar bases, where people and instruments are protected from micrometeorites and cosmic ray radiation, and the thermal conditions are stable. Recently, vertical holes were discovered in the lunar surface image data acquired by the high-resolution Terrain Camera onboard SELENE (Kaguya). The holes are possible entrances to subsurface lava tubes. However, whether lava tubes really exist underground on the Moon is still unknown.

We here report the results of our investigation of subsurface lava tube existence using the SELENE Lunar Radar Sounder (LRS) data. We first explored LRS echo wave data obtained near the Marius Hills Hole (MHH) on the “rille-A” in the Oceanus Procellarum of the Moon, and found a reflection peak signature after a sharp drop in echo power, which possibly indicates the existence of a subsurface void such as a lava tube. Then, we expanded the investigation area to 13-15°N and -58.25-55.75°E, including the MHH, and discovered several locations where the LRS echoes show similar wave patterns to that seen at the point near the MHH. We note that four of them are identified along the rille-A and on the extension of the rille, and are also on a long, narrow, sinuous mass deficit found in the GRAIL data.

The present result suggested that subsurface lava tube do exist in the vicinity of MHH, because of discovered wave patterns correspond to the existence of a subsurface lava tube.

Keywords: Lunar Radar Sounder, Lava tubes, Marius Hills Hole, SELENE

Composition of olivine-bearing rocks and their estimated origin

*Makiko Ohtake[1], Satoru Yamamoto[2], Yoshiaki Ishihara[1], Ryosuke Nakamura[3], Tsuneo Matsunaga[2]

1. Institute of Space and Astronautical Science, Japan Aerospace Exploration Agency, 2. National Institute for Environmental Studies, 3. National Institute of Advanced Industrial Science and Technology

Introduction: Remote sensing data obtained by the SELENE (Kaguya) Spectral Profiler (SP) found exposures with olivine-rich spectral features, globally distributed on the lunar surface[1], and it was suggested that they are possibly originated from the mantle.
Previous studies of returned lunar samples and the lunar magma ocean differentiation model indicate that olivine-rich rocks have the following three major origins: 1) mantle material, 2) volcanic material with olivine-rich composition, and 3) crustal material including rocks intruding into the crust (troctorite) [2]. Though most of the olivine exposures identified in [1] were located near basin rings, the origins of individual olivine sites may not be the same. Furthermore, no mantle material and only a small number of olivine-rich mare materials are available in the lunar sample collection. Therefore, understanding the origin of individual olivine exposures and advancing our knowledge about the distribution and composition of the three types of olivine-rich materials are important for understanding the composition and evolution of the lunar interior.
To address these issues, we geologically and morphologically investigated all of the identified olivine exposures in detail to assess the origin of each site in this study.
Methods: All of the 70 million latest calibrated reflectance spectra obtained by Kaguya SP [3] were used to re-identify olivine-rich exposures on the lunar surface by finding diagnostic absorption features of olivine around 1050 nm as described in [1]. Data of the Kaguya Multiband imager (MI) [4], Lunar Reconnaissance Orbiter Camera (LROC) [5], and SLDEM2013 (digital elevation model generated using the Kaguya Terrain Camera [6], MI, and Lunar Orbiter Laser Altimeter aboard LRO) of each of the identified olivine sites were used to evaluate reflectance, space weathering, geologic context, distribution and size of the exposures, composition, surface texture, and local slopes.
Results: About 150 SP reflectance spectra were re-identified as having unambiguous olivine-rich absorption features. Locations of the spectra were grouped into 50 sites located within the same latitude and longitude. We also evaluated the origin of all grouped sites. Note that we identified the clearest olivine-rich spectra among SP datasets, therefore olivine-rich material with less clear spectra may be present at other areas. We categorized their origins as likely mantle, volcanic, crustal, and “unclear”. About 60% of the sites are estimated to be mantle origin, and 5% are volcanic, 30% are crustal, and 5% are of unclear origin respectively. Mantle origin sites surround large basins whereas volcanic origin sites are within mare, and crustal origin sites are either surround or far from large basins.
Discussion: Though the percentage of each origin is not necessarily proportional to the volumes (surface area) of each category, at least there are many olivine sites of mantle origin around Crisium, Imbrium, and Nectaris. Estimation of excavation depth of these basins indicates it is likely they reach the mantle, which is consistent with the estimation of mantle origin for these olivine sites. We also identified volcanic olivine-rich sites, which have not been reported previously.
References: [1] Yamamoto et al. (2010), *Nature GeoSci.* 3, 533-536. [2] Shearer et al. (2015), *Meteorit. Planet. Sci.*, 50, 1449-1467. [3] Matsunaga et al. (2008), *Geophys. Res. Let.*, 35, L23201. [4] Ohtake et al. (2009), *Nature* 461, 236-240. [5] Robinson et. al. (2010), *Space Sci. Rev., 150*, 81-124. [6] Haruyama et al. (2009), *Science,* 323, 905-908.

Keywords: Moon, mantle, Kaguya

High resolution lunar mineral maps using Kaguya Multiband Imager data

*Paul G Lucey[1], Myriam Lemelin[2], Makiko Ohtake[3], Sarah Crites[3], Satoru Yamamoto[4]

1. Hawaii Inst Geophys & Planetol, 2. York University, 3. Japan Aerospace Exploration Agency, 4. National Institute for Environmental Studies

We determined the abundance of olivine, low-calcium pyroxene, clinopyroxene and plagioclase for the entire lunar surface at ~80 m/pixel (512 ppd) using 1°x1° mosaics of the Multiband Imager reflectance data [1,2] corrected for the shading effects of topography (MAP level 02 [2]) and Hapke's radiative transfer equations. We constructed a spectral lookup table of the reflectance spectra of 6601 mixtures of olivine, low-calcium pyroxene, clinopyroxene and plagioclase, at 7 amounts of submicroscopic iron (SMFe), an Mg# (Mg/Mg+Fe) of 65, and a grain size of 17 microns. We also modeled the reflectance spectra of these mixtures for a grain size of 200 μm for plagioclase to account for the band depth observed in the Multiband Imager data [4], for a total of 92,414 spectra. We compared the modeled spectra that contained ±2 wt% FeO of a given pixel [5], and assigned the composition to the best spectral match (in terms of correlation and absolute difference in continuum removed reflectance). We then validated the mineral abundances we obtained with global elemental maps from Lunar Prospector [6]. We also produced global maps of FeO using the algorithm of Lemelin et al. [5], and global maps of OMAT based on the algorithm of Lucey et al. [7].

The mineral maps obtained using the Multiband Imager data shows some notable differences with the mineral maps obtained using Clementine data [1]. The Multiband Imager data suggests there is much more low-calcium pyroxene than what Clementine suggested, and that low-calcium pyroxene is by far the dominant mafic mineral found in the South Pole-Aitken basin. The data also suggests that Mare Serenitatis contains much more olivine than Mare Tranquilitatis, in agreement with Mare Serenitatis having excavated mantle material [8]. The highest olivine abundances (~25 wt.%) are found in the Procellarum KREEP Terrane. High abundances (~50 wt.%) of low-calcium pyroxene and clinopyroxene are also found in the Procellarum KREEP Terrane and in Mare Tranquilitatis. Plagioclase abundances are very high in the Feldspathic Highland Terrane, but mature surface should be analyzed with caution. Indeed, there is currently a mineral identification for every pixel in the Multiband imager data. However, mature surfaces exhibit subdued absorption bands, which can lead to an overestimation in plagioclase abundances, even though we included the presence of SMFe in our modeling. Therefore, the mineral maps presented herein should be interpreted with the aid of the OMAT map. Also, we provide global mineral maps for the complete range of latitudes, but the Multiband Image data has been better calibrated within 50° in latitude [5], therefore caution should be taken when interpreting regions at higher latitudes.

References: [1] Kodama S, Ohtake M, Yokota Y, Iwasaki A, Haruyama J, Matsunaga T, Nakamura R, Demura H, Hirata N, Sugihara T, Yamamoto Y. Space science reviews. 2010 Jul 1;154(1-4):79-102. [2] Ohtake, M. et al. (2008) EPS, 60, 257-264. [3] Haruyama, J. et al. (2008) EPS, 60, 243-255. [4] Ohtake, M. et al. (2009) Nature, 461, 236-241. [5] Lemelin, M. et al. (2015) JGR, 120, 869-887. [6] Prettyman et al. 2006. [7] Lucey, P.G. et al. (2000) JGR, 105(E8), 20,377-20,386. [8] Miljkovic, K. et al. (2015) EPSL, 409, 243-251.

Keywords: Lunar, Mineral, map

Abundance and characteristics of impact melt on lunar crater central peaks

*Sarah Crites[1], Makiko Ohtake[1], Paul Lucey[2], Junichi Haruyama[1], Myriam Lemelin[3]

1. Japan Aerospace Exploration Agency, Institute of Space and Astronautical Science (JAXA/ISAS), Japan, 2. Hawaii Institute of Geophysics and Planetology, University of Hawaii at Manoa, USA, 3. Department of Earth and Space Science and Engineering, Lassonde School of Engineering, York University, Canada.

The Moon’s crust has been penetrated and modified by impact craters of all sizes over its history, ranging from micron-sized pits to basins thousands of kilometers in diameter. These craters provide a valuable three-dimensional view of the lunar crust by exposing material from depth, making material from throughout the crustal column and perhaps even the lunar mantle accessible to remote sensing observations. However, the same cratering processes that expose subsurface material also act to obscure the true local composition by contributing to extensive mixing of the surface at all scales and by producing impact melt, even on the steep slopes of central peak craters (e.g. Ohtake et al., 2009, Dhingra et al., 2016)

Taking two central peak craters (Jackson and Tycho), we isolate impact melt regions on and off the central peaks using the geologic maps of Dhingra et al. (2016) and analyze their spectral, compositional, and physical properties utilizing datasets from the Kaguya Multiband Imager (MI) and Terrain Camera (TC), the LROC Narrow Angle Camera (NAC), and the Diviner Lunar Radiometer.

Consistent with previous work (Ohtake et al., 2009; Kuriyama et al., 2012), we find that the regions of Jackson’s central peak identified as impact melt are compositionally distinct, with higher iron (avg. FeO 5%) and lower modeled plagioclase content (avg. plagioclase 79%) than the rest of the very plagioclase-rich central peak (avg. FeO 2%, avg. plagioclase 90%). This indicates that for central peaks like Jackson with substantial impact melt, it is important to exclude melt from compositional analyses to understand the true local composition. However, the impact melts mapped on Tycho’s central peak are not substantially different in iron content than the average central peak (both average 6% FeO).

While detailed geologic maps based on high resolution imagery such as Kaguya Terrain Camera or LROC Narrow Angle Camera are an effective tool for eliminating potentially contaminated regions of central peaks, this approach is time consuming and subjective. For large-scale surveys, a quantitative metric for narrowing data to areas less affected by mixing and contamination is needed in order to ensure only the most reliable spectra are interpreted. We investigated three possible discriminators (LOLA/TC slope, Diviner rock abundance, optical maturity) for identifying fresh and uncontaminated surfaces, and find that rock abundance may be a promising metric.

The rock abundance of the impact melt deposits on Jackson’s central peak is very low, with average rock fractions near 0.03, in contrast to the rest of the central peak, which has an average rock abundance of 0.056. The rock abundance distributions for the melt regions both on and off the central peak are also skewed strongly to the right, with skewness values greater than 1, whereas the average central peak and mapped boulder regions have skewness values below 1. The slopes and optical maturity values for the impact melt units vary, and do not appear to provide a diagnostic measure of the presence of melt.

While our analysis suggests that rock abundance is an effective discriminator of impact melt, at least for

Jackson crater, it may only be applicable to central peak craters within a certain age range, as older craters have much lower rock abundances, and regolith development throughout the central peak might mask the anomalously rock-free signature of melts. Efforts are underway to map impact melt on older central peaks and compare melt rock abundance distributions with average central peak values for these more weathered craters.

Ohtake, M. et al. (2009) *Nature, 461*, 236-241. Kuriyama, Y. et al. (2012) *LPSC 43*rd, Abstract #1395.
Dhingra, D. et al. (2016) *Icarus, 000,* 1-14.

Keywords: Moon, Impact Processes, Central Peaks, Spectroscopy, Kaguya, Lunar Reconnaissance Orbiter

Global classification map of lunar absorption spectra and new impression of lunar crust formation.

*Makoto Hareyama[1], Yoshiaki Ishihara[2], Hirohide Demura[3], Naru Hirata[3], Chikatoshi Honda[3], Shunichi Kamata[4], Yuzuru Karouji[5], Jun Kimura[6], Tomokatsu Morota[7], Hiroshi Nagaoka[8], Ryosuke Nakamura[9], Satoru Yamamoto[10], Yasuhiro Yokota[11], Makiko Ohtake[2]

1. St. Marianna University School of Medicine, 2. Japan Aerospace Exploration Agency, 3. The University of Aizu, 4. Hokkaido University, 5. Tokyo Metropolitan University, 6. Osaka University, 7. Nagoya University, 8. Waseda University, 9. National Insitute of Advanced Science and Technology, 10. National Institute for Environmental Study, 11. Kochi Unicersity

This report presents the global classification map of lunar absorption spectra by unsupervised classification methods and new impression of lunar crust formation based on the map.
Geologic map is an important tool to understand formation process of lands. Many Moon’ s geologic maps has been made by many researchers based on their own criteria. Therefore we are hard to compare different sites on the Moon far from each other.
In order to solve such problem, the study of making global geologic map of the Moon has been started 3 years ago, and we made the global classification map of lunar absorption spectra based on hyper spectrum data of Spectral Profiler/Kaguya. Since this map was produced by both K-means and ISODATA of unsupervised classification methods under unified criteria for whole Moon, we can easily compare a region with others far from there.
The entire Moon was divided into 66 classes of lunar absorption spectra. The entire Moon was divided into 66 classes of lunar absorption spectra by unsupervised classification methods and those were categorized as 5 regional groups based on major corresponding location, which were Mare (M) group, Highland (H) group, South Pole-Aitken (S) group, Boundary between groups of M/S and H (B) group and Ejecta from fresh highland craters (E) group.
Some local class distributions showed good agreement with past those such as Aristarchus region, Orientale region, SPA region and highland region. Also, it was found that some area of B group covered cryptomaria and some spectrum classes corresponded to craters itself in maria and highland region. Furthermore, some new impressions of the lunar crust formation related to cryptomaria and/or layer structure of subsurface were found through comparison of different sites far from each other based on the presenting global map.

Keywords: Moon, geologic map, crust formation

Near-Far Asymmetry of Magma Production and Conditions of Magma Eruption of the Moon: Constraints from Mare Volumes within the Impact Basins

Masako Taguchi[1], *Tomokatsu Morota[1], Shinsuke Kato[1]

1. Graduate School of Environmental Studies, Nagoya University

To understand the thermal conditions of the lunar mantle and its lateral heterogeneity, estimates for volumes of mare basalts are essential. However, because of the absence of high-resolution remote sensing data on the lunar farside, accurate volume estimates of farside maria had been limited until recently. In this study, we estimated the volumes of mare basalts within five farside basins, Apollo, Ingenii, Poincare, Freundlich-Sharonov, and Mendel-Rydberg, and one nearside basin, Crüger-Sirsalis, using topographic and multiband image data obtained by SELENE (Kaguya). Furthermore, using the high-resolution crustal thickness model constructed from GRAIL gravity data and LRO topography data, we investigated the crustal thickness of major impact basins and the relationship with the magma eruption. The results of volume estimates indicate that farside mare volumes are ~100 times smaller than those of the nearside. From a relationship between the mare volumes and the crustal thicknesses of each basin, it was also found that the minimum crustal thicknesses within the basins were a dominant factor that determined whether magma erupted at the surface and that the critical crustal thickness for magma eruption were ~12 km for the farside and ~20 km for the nearside. In the areas with thinner crust than the critical thicknesses, the total mare volumes do not depend on the crustal thickness. These results suggest that the lunar diapirs had typical sizes for the nearside and the farside, respectively. The diaper radii were estimated to be 3.5–4.4 km for the nearside and 2.2–3.3 km for the farside based on a simple magma ascent model considering the balance of the positive buoyancy of the diaper at the crust-mantle boundary and the negative buoyancy of a dike in the crust. The ratio in the diaper volumes between the nearside and the farside is only 2.6–4.0, much smaller than the observed ratio of mare volumes (100 times). Therefore, the observed ratio of mare volumes should be explained by difference in frequencies of magma eruption. The eruption frequencies were calculated to be 200–3000 for the nearside and 10–200 times for the farside based on the observed total volumes of mare basalts. Furthermore, from the estimated diaper sizes and eruption frequencies, we estimated that magma production in the farside mantle might be ~15-20 times smaller that of the nearside mantle. This result implies a stronger near-far dichotomy than previously estimated.

Keywords: Moon, Mare volcanism, Lunar dichotomy, Mare basalt, Crustal thickness

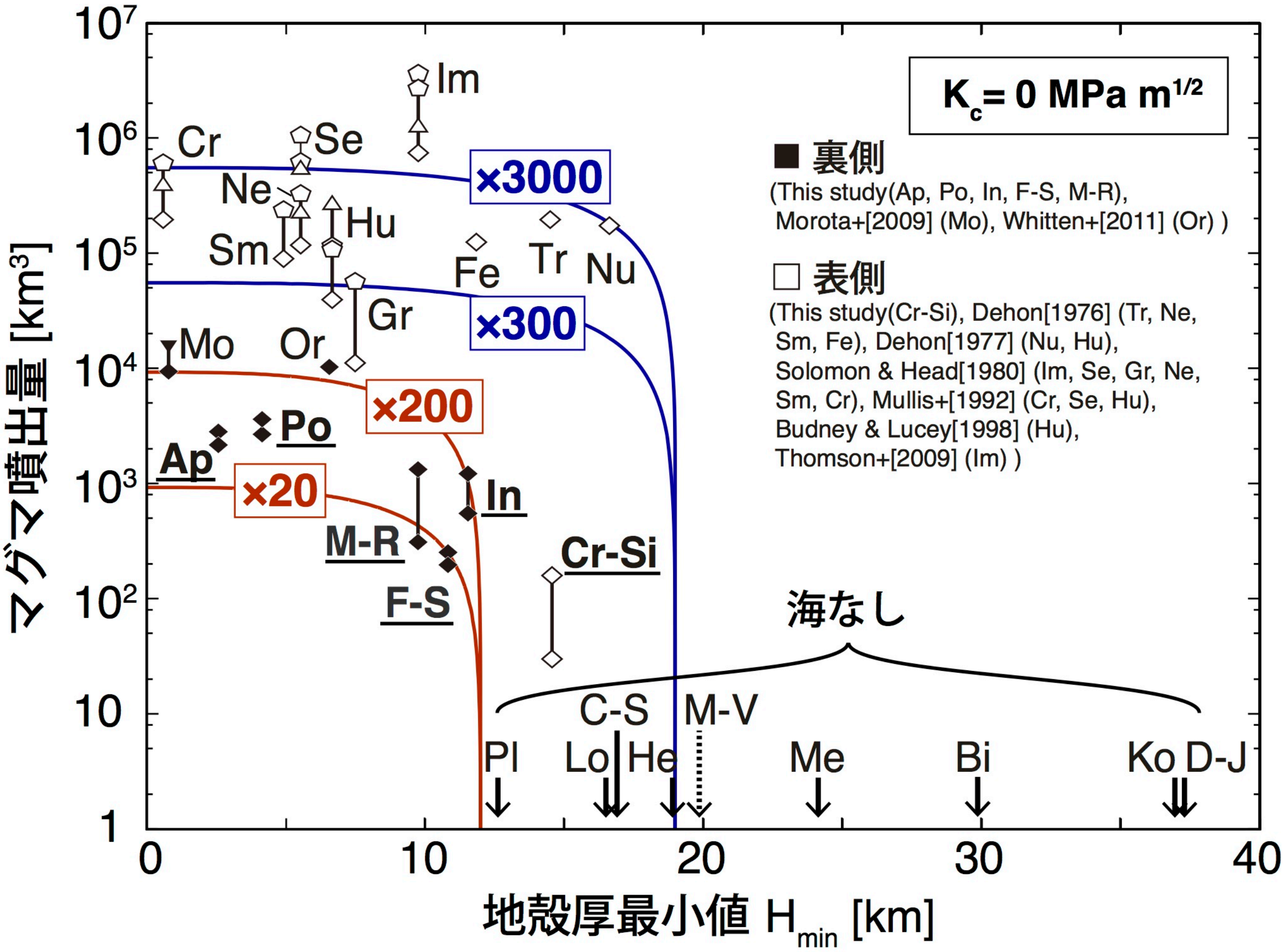

K_c= 0 MPa $m^{1/2}$
■ 裏側
(This study(Ap, Po, In, F-S, M-R), Morota+[2009] (Mo), Whitten+[2011] (Or))
□ 表側
(This study(Cr-Si), Dehon[1976] (Tr, Ne, Sm, Fe), Dehon[1977] (Nu, Hu), Solomon & Head[1980] (Im, Se, Gr, Ne, Sm, Cr), Mullis+[1992] (Cr, Se, Hu), Budney & Lucey[1998] (Hu), Thomson+[2009] (Im))
×3000
×300
×200
×20
Im
Cr
Se
Ne
Hu
Sm
Fe
Tr
Nu
Gr
Mo
Or
Po
Ap
In
M-R
F-S
Cr-Si
海なし
C-S
M-V
Pl
Lo
He
Me
Bi
Ko
D-J
マグマ噴出量 [km^3]
地殻厚最小値 H_{min} [km]

Characteristics of mineral compositions of lunar late mare volcanism revealed from Kaguya data

*Shinsuke Kato[1], Tomokatsu Morota[1], Yasushi Yamaguchi[1], Sei-ichiro WATANABE[1], Hisashi Otake[2], Makiko Ohtake[2], Tokuhiro Nimura[3]

1. Nagoya University Graduate School of Environmental Studies, 2. Japan Aerospace Exploration Agency, 3. Japan Spaceguard Association

In order to understand the crystallization of lunar magma ocean and following evolution of the lunar mantle, reconstructing the volcanic history of the Moon is important. The relation between compositions and ages of lunar mare basalts provides insights into the compositional structure and the thermal history of the lunar mantle. According to previous studies of crater counting analysis using remote sensing data, the age distribution of mare basalts shows a second peak at ~2 Ga, which concentrated in the Procellarum KREEP Terrane (PKT). To understand the mechanism for causing the second peak and its magma source is essential to constrain the thermal history of the moon.
In our previous study, we investigated the relation between eruption ages and titanium contents of mare basalts. As a result, we found that a rapid increase in mean titanium content occurred near 2.3 Ga, suggesting the magma source transition. Moreover, the high-titanium basaltic eruptions are correlated with the second peak in volcanic activity at around 2 Ga. We designate volcanisms before and after 2.3 Ga as Phase-1 and Phase-2 volcanism. We propose that Phase-2 volcanism can be explained by the three possible scenarios: (1) the ilmenite-bearing cumulate rich layer in the core-mantle boundary formed after the mantle overturn, (2) the basaltic material layers beneath the lunar crust formed through upwelling magmas, and (3) ilmenite-bearing cumulate blocks remained in the upper mantle after the mantle overturn. We also searched the evidence of the magma source transition in topographic features. As a result, we found a feature like a plateau in the central region of the PKT where most of Phase-2 mare basalts erupted, suggesting that the origin of the plateau might be related to Phase-2 volcanism.
To understand the magma source transition around 2.3 Ga, reconstructing the history of the volcanic activity in the PKT is essential. In this study, we focused on the central region of the PKT and make new geological map of this region. Then, we performed spectral analysis of mare basalts to investigate mineral compositions of mare basalts. At first, we made geological map of the central region of the PKT using KAGYA Multiband Imager (MI) data and digital terrain model (DTM) derived from KAGUYA Terrain Camera data and investigated mineral compositions of mare basalts using KAGYA Spectral Profiler (SP) data. We calculated absorption depths of 950, 1050 and 1250 nm reflectance data from MI to divide highland and mare regions in the central region of the PKT. Also, topographic roughness was calculated from DTM to identify highland regions. We performed principal component analysis for MI 8 band reflectance data to identify each mare basalt unit.
To deconvolute an observed spectrum into individual mineral components, the modified Gaussian model (MGM) is generally used. However, it is difficult to fit the spectrum of complicatedly mixed material such as mare basalts by the MGM because each mineral has multiple absorption bands. Nimura (2011) improved the MGM by investigating the relations between chemical compositions of minerals (the ratio of Fe/(Fe+Mg) in olivine and the ratios of Ca/(Ca+Fe+Mg) and Fe/(Ca+Fe+Mg) in pyroxene) and absorption band parameters (center, width and strength ratio of Gaussian curves). This method was applied to the spectra of asteroids in the previous study and successfully could model mineral and chemical compositions. In this study, we applied this method to the spectra of mare basalts obtained by KAGUYA SP. To avoid the effect of the space weathering, we used spectra of fresh crater wall.
At present, we enhanced the field of the geological map of the PKT and we are performing spectral

analysis of mare basalts. In this presentation, we show the updated geological maps of the PKT and the result of spectral analysis of Phase-1, Phase-2 mare basalts in the Oceanus Procellarum and Mare Tranquillitatis.

Keywords: Moon, volcanism, mineral composition, spectrum

Re-evaluation of deep moonquake source parameters and implication for thermal condition of deep lunar interior.

*Taichi Kawamura[1], Philippe Lognonné[2], Yasuhiro Nishikawa[2,4], Satoshi Tanaka[3]

1. National Astronomical Observatory of Japan, 2. Institut de Physique du Globe de Paris, 3. ISAS/JAXA, 4. University of Tokyo

While deep moonquakes are seismic events commonly observed on the Moon, their source mechanism is still unexplained. The two main issues are poorly constrained source parameters and incompatibilities between the thermal profiles suggested by many studies and need for brittle properties at these depths. In this study, we reinvestigated the deep moonquake data and uncover the atypical feature of deep moonquake that completely differs from those of the Earth. We first improve the estimation of source parameters through spectral analyses using virtual "new" broadband seismic records made by combining those of the Apollo long and short period seismometers. We use the broader frequency band of the combined spectra to estimate corner frequencies and DC values of spectra, which are important parameters that constrain the source mechanism. We use the spectral features to estimate seismic moments and stress drops from 3 deep moonquake source regions. Secondly, we show that the large strain rate from tides makes the use the new sets of source parameter and re-evaluate brittle-ductile transition temperature at deep moonquake source regions. We finally take the temperature as an additional constraint and estimate the temperature profile that is compatible with deep moonquake occurrence and other geophysical observations such as surface heat flow measurements and geodetic observations.

Keywords: Lunar Science, Seismology, Planetary Science

Re-determination of lunar crustal thickness around the Apollo landing site by analyzing Apollo artificial impacts' seismic data combined with LRO's products

*Keisuke Onodera[1,2], Satoshi Tanaka[2], Taichi Kawamura[3], Yoshiaki Ishihara[2]

1. SOKENDAI (The Graduate University for Advanced Studies), 2. JAXA/ISAS, 3. NAOJ

It has been about 50 years since the seismometers were deployed on the Moon in the Apollo missions. Since then, some topics have been studied by analyzing the lunar seismic data. For example, core size, composition of the Moon, velocity structure of the lunar interior and so on. The lunar internal structure gives us important information about origin and evolution of the Moon. For instance, we can estimate bulk abundance of Al from lunar crustal thickness and it gives constraints for the lunar formation. In the previous lunar seismic analyses, the artificial impacts were often used to constrain the lunar crustal thickness because of known source locations and impact times from the tracking of the impactors. Five S-IVB rocket boosters and four Lunar Module impacts were deliberately impacted on the surface of the Moon to generate the seismic waves. All of them were succeeded to track except for Apollo 16 S-IVB booster. Loss of radio contact between the Apollo 16 S-IVB left large uncertainties on the location of the impact. However, the precise source locations of the five S-IVB impacts were updated with Lunar Reconnaissance Orbiter(LRO) image data recently. The updated locations resulted in change in the reference source locations for the travel time analysis with these artificial impacts. Especially, as for Apollo 16 S-IVB, we found that its impact site estimated in Apollo era was different from the precise one by about 30 km. In this study, we re-analyzed artificial impacts' seismic data using the precise source locations to determine more accurately the crustal thickness of the Moon. We will present the crustal thickness around the Apollo landing site and discuss the effect of local structure that might affect the travel time analyses. We will also discuss implications for future lunar seismic exploration for better understandings of lunar crustal structure.

Keywords: Moon, Apollo lunar seismic data, Lunar interior exploration, LRO

Studies for the source region of lunar basaltic brecciated meteorites, Northwest Africa 773 group on the geochemical, mineralogical and petrological analyses

*Hiroshi Nagaoka[1], Timothy Fagan[1], Masahiro KAYAMA[2], Nobuyuki Hasebe[1], Yuzuru Karouji[3], Mitsuru Ebihara[3], Makiko Ohtake[4]

1. Waseda University, 2. Tohoku University, 3. Tokyo Metropolitan University, 4. Japan Aerospace Exploration Agency

Lunar meteorites originate from craters that are randomly distributed on the surface and thereby provide valuable information on geochemistry, mineralogy, and petrology of the source regions that are not obtained from the Apollo and Lunar mission samples. The recent-improved remote sensing data (e.g., Kaguya, LRO, Chandrayaan-1) are very powerful tool to interpret their source regions. Identification of the source region of lunar meteorite could be almost equivalent to the sample return from that region. Lunar meteorites, Northwest Africa (NWA) 773 clan consist of a group of paired meteorites with different lithologies (NWA 773, 2727, 2977, 3160, 3333, 6950, and more). Some of them contain olivine cumulate gabbro (OC) as lithic clasts in a basaltic breccia, while NWA 2977 and NWA 6950 entirely consist of OC. Furthermore, NWA 773 clan contains a variety of clasts other than OC: olivine phyric basalt, pyroxene phyric basalt, pyroxene gabbro, ferroan symplectite, alkali-rich phase ferroan rocks, and silicic rock. Such a variable lithological types indicated the complex igneous petrogenesis and subsequent brecciation of the source region of NWA 773 clan. In this work, the geochemical, mineralogical and petrological characteristics of their source region were discussed by comparing the lunar sample and Kaguya observational data.
Lunar meteorites, Northwest Africa 773 clan were investigated with geochemical, mineralogical and petrological microanalyses: 1) the bulk chemical compositions were obtained by neutron-induced prompt gamma-ray analysis (PGA) and instrumental neutron activation analysis (INAA) in the Japan Atomic Energy Agency; 2) mineralogical and petrological data of NWA 773 clan were investigated by Scanning Electron Microscope (SEM) and Electron Prove Micro-Analyzer (EPMA) at Waseda Univ., visible and near-infrared reflectance spectra obtained by a JASCO reflectance spectrometer at JAXA; 3), where their radiogenic ages were discussed by references of several literatures.
Rare Earth Element (REE) compositions from NWA 773 breccia have similar KREEP-enriched patterns of their light-REE-enriched and heavy-REE-depleted patterns, and negative Eu anomaly. The NWA 773 clan breccias show the wide range REE values among each portion of NWA 773 clan breccias (La = 40 –170 × CI chondrite), which probably reflects variable abundances of KREEP-rich clasts in the breccia. In fact, we observed an evolved igneous clast (high-silica) in NWA 2727 breccias. Silica-rich rocks (e.g., felsite, granite) from the Apollo missions are highly enriched in incompatible elements (REE, K, Th).
NWA 773 clan represents the following characteristics: 1) the included igneous clasts derived from basaltic to rhyolitic magma composition on the Moon, 2) NWA 773 clan breccias represent high-Th (max 5.15 μg/g), -FeO (>15wt%), and very-low-Ti (<1wt%) composition, 3) the included OC lithologies represent one of youngest crystallization ages (3 Ga) among lunar samples. The first suggests that the silica-rich rocks in NWA 773 clan could be associated with putative silicic volcanism observed by the recent remote sensing data. The above features of NWA 773 clan were permitted in Procellarum KREEP Terrane (PKT), as putative silicic volcanism mostly occurs in PKT. NWA 773 clan allows us knowledge of complex igneous activities in PKT. Furthermore, the source region of NWA 773 clan will be narrowed down within PKT region by comparing with the following data: 1) bulk FeO, CaO, TiO_2, K, Th contents of NWA 773 clan breccia vs. elemental distribution maps obtained by Kaguya gamma-ray spectrometer; 2)

visible and near-infrared reflectance spectra of NWA 773 clan vs. reflectance spectra obtained by Kaguya spectral profiler, 3) the crystallizaition ages of NWA 773 clasts vs. the eruption ages obtained by Kaguya Terrain Camera. As described here, the source regions can be well interpreted on the basis of the combination of data from lunar meteorite and remote sensing observations.

Keywords: meteorite, KREEP, volcanism

Moganite in lunar meteorite, Northwest Africa 773 clan: Trace of H_2O Ice in the Moon’s Subsurface

*Masahiro KAYAMA[1,2], Naotaka Tomioka[3], Eiji Ohtani[1], Yusuke Seto[4], Hiroshi Nagaoka[5], Jens Götze[6], Akira Miyake[7], Shin Ozawa[1], Toshimori Sekine[8,9], Masaaki Miyahara[8], Kazushige Tomeoka[4], Megumi Matsumoto[4], Naoki Shoda[4], Naohisa Hirao[10]

1. Department of Earth and Planetary Material Sciences, Faculty of Science, Tohoku University, 2. Creative Interdisciplinary Research Division, Frontier Research Institute for Interdisciplinary Sciences, Tohoku University, 3. Kochi Institute for Core Sample Research, Japan Agency for Marine-Earth Science and Technology, 4. Department of Planetology, Graduate School of Science, Kobe University, 5. Research Institute for Science and Engineering, Waseda University, 6. TU Bergakademie Freiberg, Institut für Mineralogie, 7. Department of Geology and Mineralogy, Graduate School of Science, Kyoto University, 8. Department of Earth and Planetary Systems Science, Graduate School of Science, Hiroshima University, 9. Center for High Pressure Science and Technology Advanced Research, 10. Japan Synchrotron Radiation Research Institute

Lunar water locally concentrates as a result of the migration of H_2O molecules on the sunlit surface towards the colder regions. The molecular water is subsequently cold-trapped as ice on the permanently shadowed regions, the poles and theoretically Moon’s subsurface. Although a few trace of subsurface H_2O has been observed by remote sensing spectrometers (e.g., LCROSS), it has not been reported in the Apollo and Luna samples and lunar meteorites yet. In this study, lunar meteorites, the Northwest Africa (NWA) 773 clan, were investigated and thereby moganite, a monoclinic SiO_2 phase precipitated from alkaline fluids, was discovered by various microanalyses. A formation process of this lunar moganite was also interpret to evaluate origin of the Moon’s subsurface H_2O.

Lunar meteorites of the NWA 773 clan were selected for Raman spectroscopy, electron microscopies and synchrotron X-ray diffraction (SR-XRD). The KREEP-like NWA 773 clan commonly consists of gabbroic and/or basaltic clasts.

Silica occurred as anhedral micrograins between the constituent minerals in the lunar meteorite. Raman spectra of the silica micrograins exhibited pronounced peaks at 128, 141, 217 and 503 cm^{-1}, which corresponded to those of moganite. Coesite Raman peaks were also identified together with the moganite signature. Raman intensity mapping revealed that the silica micrograins contain abundant moganite in its core, surrounded by coesite. SR-XRD of several silica micrograins also confirmed moganite and coesite. Transmission electron microscopy clarified that the silica micrograins consist of nanocrystalline particles with an average radius of 4.5 nm. Most of the SiO_2 nanoparticles were identified as moganite by selected area electron diffraction (SAED) patterns. Moganite was accompanied by small amounts of coesite, according to SAED analyses of the SiO_2 nanoparticles.

Moganite-bearing silica micrograins in the NWA 773 clan precipitated from lunar alkaline fluids rather than terrestrial weathering for the following reasons: (1) Occurrence only in a part of the NWA 773 clan. (2) Moganite surrounded by the coesite rim. (3) High moganite content contradicting reduced content to <20 wt% under dry desert condition over terrestrial age.

A formation process for lunar moganite can be explained as follows. A host gabbroic and basaltic rock of the NWA 773 crystallised within the Procellarum KREEP Terrene (PKT). Subsequently, carbonaceous-chondrite collisions occurred on the surface of the PKT, followed by ejection of the host rock due to the impact events. The alkaline water delivered by the carbonaceous chondrite was captured as a fluid during the brecciation on the impact basin. Below the freezing point, this fluid got cold-trapped as H_2O ice in the subsurface. Simultaneously, the moganite-rich silica micrograins precipitated from the captured alkaline fluid on the sunlit surface. The NWA 773 clan was launched from the PKT by the latest

impact event, thus producing transformations to coesite from moganite.

Keywords: Lunar meteorite, Moon, Subsurface water, H2O ice

Origin and evolution of Moon

*Shigenori Maruyama[1]

1. Earth-Life Science Institute, Tokyo Institute of Technology

The ABEL model, newly proposed to discuss the history of the Moon. The core of this new model is characterized by two steps:(1) a Dry-Earth Moon system formed at 4.53Ga, and (2) ABEL Bombardment, which delivered volatiles to the Moon’ s interior and atmospheric and oceanic components to the Earth at 4.37-4.20 Ga with the minor bombardment continuing up to 3.9 Ga. During the ABEL Bombardment, asteroids bombarded the nearside of the Moon, selectively causing frictional mantle heating down to the deep mantle. The largest impact at around 4.37 Ga resulted in such effect even at Aitken on the opposite side of the Moon through mantle to the surface, which included the transferal of volatiles into the deep mantle and lowering the viscosity of the hydrated mantle. About 200 million years after the bombardment, the mantle rebounded upwards to generate a series of basalts within the craters. This kind of rebound did not occur on the farside because bombardment was less on the farside.
A new model of the history of the Moon includes the following seven major events: (1) giant impact to form the Moon-Earth system;(2) formation of a magma ocean and its consolidation; (3) injection of water into the Moon through 4.37-4.20 Ga ABEL Bombardment;(4) widespread isostatic-rebound magmatism over the Procellarum KREEP Terrane (PKT) on the nearside Moon (extension on the nearside caused compression on the farside by thrusting); (5) strong magnetism;(6) Copernican bombardment; and (7) gaseous eruption combined with Moonquakes up to now.

Keywords: ABEL Model, Geology of Moon, secondary accretion of volatiles

The heterogeneities in Lunar interior: Role of High Titanium materials

*Eiji Ohtani[1], Mako Igarashi[1], Tatsuya Sakamaki[1], Dapeng Zhao[2]

1. Department of Earth and Planetary Materials Science, Graduate School of Science, Tohoku University, 2. Department of Geophysics, Graduate School of Science

Tomographic images of the lunar mantle have been reported by Zhao et al. (1) using the Apollo seismic data. They reported existence of P and S-wave anomalies in the lunar mantle which could relate also to the epicenters of the deep moonquakes. There is a possibility that the cause of the lunar P and S-wave anomalies is completely different from that of the Earth's mantle. In the Earth, slow seismic anomalies are the signature of hot plumes ascending in the Earth's mantle. On the other hand, the seismic anomalies in lunar mantle may be caused by compositional heterogeneities. Elkins-Tanton et al. (2) presented a model of solidification of the lunar magma ocean. In their model, titanium rich cumulates were formed in the later stage of its solidification, and gravitational overturn occurred in the early Moon. This overturn provided titanium rich regions in the lunar deep interior. Some of these materials might have stagnated and could have produced chemical heterogeneities in the lunar mantle. Titanium enriched materials are denser and slower in seismic wave velocity compared to that of the normal lunar mantle, which causes slow seismic velocity anomalies. Previous measurements of density and sound velocity of Ti-rich materials and magmas (3) indicate clearly that the Ti-rich materials which are remnant of the early overturn can cause slow velocity anomalies. Igrashi et al. (4) measured the solidus temperature of the Ti enriched materials at around 3-5 GPa corresponding to the base of lunar mantle, and showed the solidus temperature is lower than the lunar geotherm, i.e., the partial melting occurs in the lunar lower mantle generating dense magmas at the depths (3). Thus, the molten high Ti melts can cause high attenuation and slow seismic velocity regions at the base of the lunar mantle. More precise seismic tomography studies of the moon and mineral physics studies of the lunar materials are essential to clarify the heterogeneities of the lunar mantle in the future lunar exploration. It is very important to separate the chemical and thermal heterogeneities in the lunar mantle and to compare the difference from those of the Earth's mantle.

References: (1) Zhao et al. (2008), Chinese Sci. Bulletin, 53, 3897-3907, Zhao et al. (2012), Global Planetary Change, 90-91, 29-36, (2) Elkins-Tanton et al. (2011), EPSL, 304, 326-336 (3) Sakamaki et al. (2010), EPSL, 299(3), 285-289, (4) Igarashi et al. (This meeting abstract)

Keywords: Tomography, High titanium material, Lunar magma ocean, Heterogeneity, lunar mantle

Possible observation of free core nutation of the moon

*Hideo Hanada[1], Masatsugu Ooe[2], Natalia Petrova[3], Alexander Gusev[3]

1. RISE Project, National Astronomical Observatory, 2. Oshu Space and Astronautical Museum, 3. Kazan Federal University

The Earth has a fluid core and it can rotate around the axis different from that of the mantle because it is fluid.
If the axis of rotation of the fluid core and that of the mantle incline a little to each other for some cause, they begin rotation around the other axis anticlockwise because forces acting on the core mantle boundary (CMB) are asymmetrical to the figure axis of the mantle. This phenomenon is called the Free Core Nutation (FCN).
In case of the Earth tides, the period of FCN is about 460 sidereal days, and when seeing on the rotating coordinate fixed to the Earth, the angular velocity becomes 1-1/460 (turns/ sidereal day), which is close to the period of 1 sidereal day.
There are a lot of components of diurnal Earth tides near the period of 1 sidereal day, and the amplitudes of these components are magnified according to the resonance of the period of FCN, which is called fluid core resonance.

Whether the Moon has a fluid core or not is still unclear although it is an important issue which is related to existence or non-existence of paleo magnetic field and thermal history of the Moon. There were researches which suggested energy dissipation inside of the Moon from the analysis of Lunar Laser Ranging data (Williams et al, 2001) and which suggested partial melting inside of the Moon from the theoretical estimation of tidal heating (Harada et al., 2014). However there has been no observation which directly show the existence of the fluid core.

The period of FCN is estimated to be from several to 20 decades according to lunar model and the amplitude is less than 16 arc seconds (Gusev et al., 2016). Astronomical observations of FCN might be very difficult because its period is too long. However observations of deformation or gravity variation affected by resonance of FCN appear on the lunar surface are more practical like the Earth. Supposing the mean angular velocity of the Moon be Ω_L, angular velocity of FCN relative to inertia space be n_L, then FCN is observed on the Moon as the angular velocity of Ω_L-$n_{L.}$ It becomes 0.0366-1 / (200×365) = 0.03660099-0.00001370=0.03658729 (27.331 days) for the period of 20 decades..

Because there are a lot of components of lunar diurnal tides around the 27.3 days, there is possibility that the amplitudes are magnified by the resonance of FCN. Not only the tidal variations but the forced physical librations which are caused by the same forces must be affected by the resonance. Actually there are some evidences of resonance in the result of analyses of Lunar ephemeris DE421 expanded to over 1000 years (Rambaux&Williams, 2010). However, there are free modes such as the precession (about 24 year period), the Chandler like polar-motion (about 75 years), the free librations (about 100 years for latitudinal mode and 2.9 years for longitudinal mode) as well as FCN (Gusev et al., 2016), and the resonance effects must be complicated.

We try to estimate the effect of resonance existence of FCN, and we propose to observe tidal deformation and gravity tides on the moon surface.

Keywords: Lunar interior, Free core nutation, Free core resonance, Lunar tides

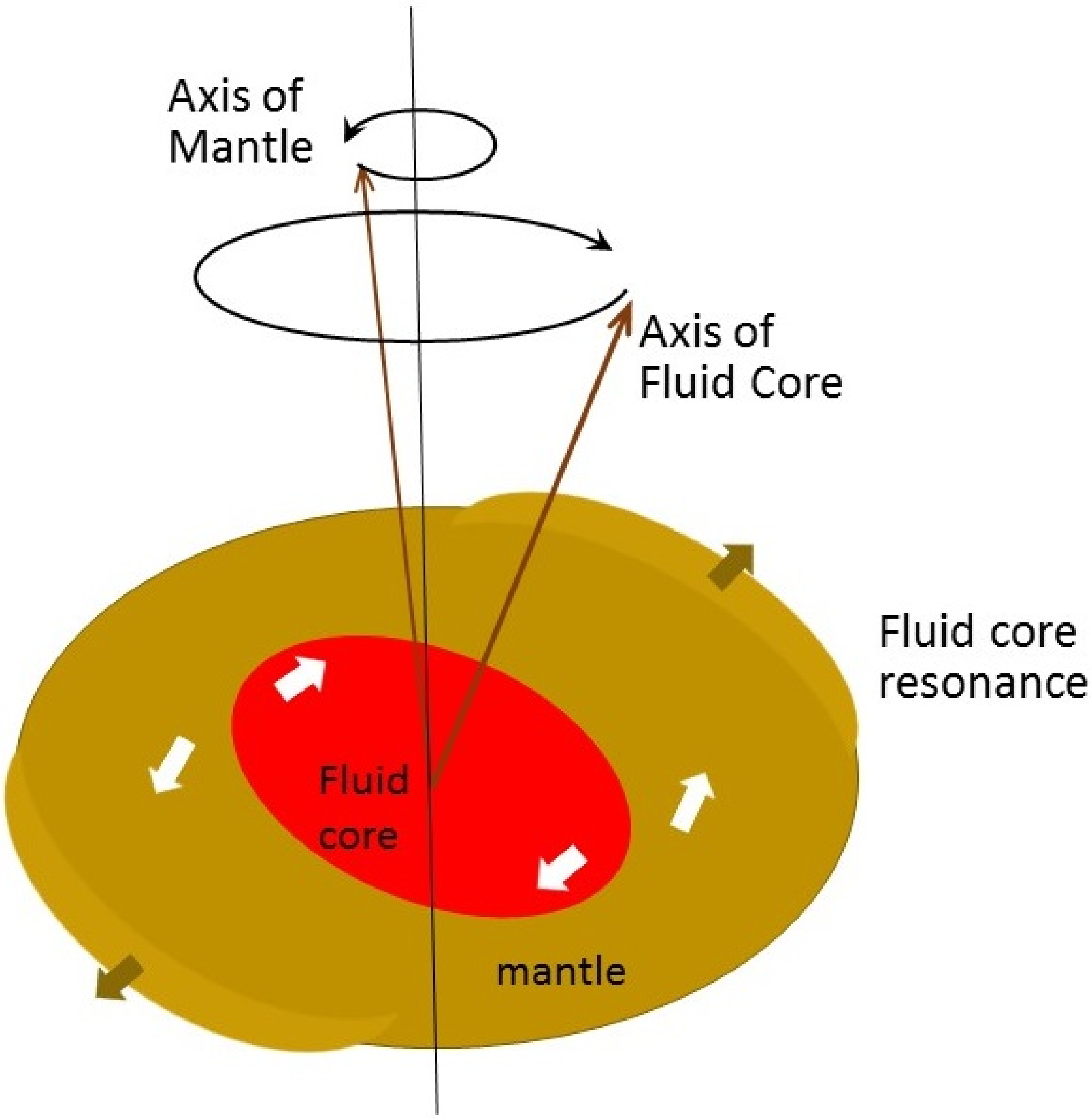

Classification of deep moonquakes using machine learning technique and application of it to lunar science and exploration

*Ryuhei Yamada[1], Kodai Kato[2], Shiori Kikuchi[2], Yukio Yamamoto[3], Masaharu Hirota[4], Shohei Yokoyama[5], Hiroshi Ishikawa[2]

1. The University of Aizu, Research Center for Advanced Information Science and Technology, 2. Tokyo Metropolitan University, 3. Japan Aerospace Exploration Agency, 4. National Institute of Technology, Oita College, 5. Shizuoka University

A lot of lunar seismic events had been observed by 4 seismic stations deployed at Apollo 12, 14 15 and 16 sites through NASA Apollo mission from 1969 to 1977. Deep moonquake which occurs at depth of about 700-1200 km is most frequent lunar seismic event, and 106 sources have been located. The deep moonquake events occurred from the located source have been analyzed to investigate the lunar deep structure (e.g., Lognonn et al., 2003, Matsumoto et al., 2015). We know that the deep moonquakes occur repeatedly related with tidal force worked on the lunar interior and the waveforms of the events generated from the same source are similar (Nakamura et al., 1982). The sources of many deep moonquake events have been identified using the similarity of the waveforms (e.g., Nakamura, 2003). On the other hand, about 20% of the discovered lunar seismic events are still unclassified and about several hundreds of the deep events are unlocated. This fact indicates that the previous identification of the deep moonquake sources using the waveform similarity is not necessarily sufficient. In the previous studies, the waveforms of deep moonquake in time series are mainly analyzed to classify the sources using the similarity (e.g., Nakamura, 2003, Bulow et al., 2005), and they would not be enough to classify the sources. Therefore, we have investigated new parameters to classify the deep moonquake sources efficiently using the supervised machine learning technique.

In this study, we analyzed the deep moonquake events occurred from the known active sources observed at Apollo12 station. Firstly, we have investigated effectivity of power spectral density (PSD) in frequency domain to classify the deep sources using one of conventional machine learning technique; Support Vector Machine (SVM). This result has shown that the PSD using 15 minutes’ data from arrival of P-wave are more effective to classify the sources compared with waveform in time series (Goto et al., 2013, Kato et al., 2016). Secondary, most effective machine learning technique for classification of the deep source has been studied, and we found that Neural Network has the best availability among five representative method. Then, it is often difficult to extract the effective parameters from the waveforms due to small amplitude and strong scattering of the waveforms. From the reason, we have investigated positional relation between the Moon and other planets at occurrence time of each deep moonquake as the parameters for the classification without using the waveforms, because it is known that deep events occur related with relative position (that is tidal force) among the Moon, the Earth and the Sun (e.g., Lammleign, 1977). This investigation has shown that relative position and velocity between the Moon and the Earth were important to identify some deep moonquake sources (Kato et al., 2017).

We found that these new parameters and method for classification of the deep sources are available to identify the source of the unlocated deep events (Kikuchi et al., 2017). Most deep moonquake source have been located in lunar near-side and there are only small number of sources in lunar far-side. However, Nakamura (2005) describes that some deep moonquake events which may occur from undiscovered far-side sources are detected at only one or two Apollo stations. Though this number is insufficient to locate the source from travel-time analysis, if we can identify that the unclassified events generate from the same far-side source and increase the observation points using our new method, we may be able to locate that and discover new far-side sources. This discovery will give new knowledge about activity of far-side deep events, internal structure in lunar far-side and the lunar dichotomy. Then, it can be expected that we can discover a lot of new deep moonquakes in sequential seismic data observed during about 7 years using the new parameters such as PSD. In future lunar seismic experiments such as SELENE-2 (Tanaka et al., 2008) and Approach (Yamada et al., 2016), we can deploy only one or two seismic stations, and the number is insufficient to locate the deep moonquakes. In this case, if we can identify the source of detected deep events using the positional relation between the Moon and other planets, we will be able to obtain new travel time data of deep moonquakes on the future missions in spite of a few seismic stations.

Keywords: Deep moonquake, Machine learning technique, Analysis of moonquake waveform, Lunar interior structure, Lunar exploration

A simulation study of Lunar Farside Lander positioning with a Four-way Lander-Orbiter Relay Tracking Mode

*Mao Ye[1], Fei Li[1,2], Jianguo Yan[1], Weifeng Hao[2], Weitong Jin[1], Xuan Yang[1], Shengkai Zhang[2]

1. State Key Laboratory of Information Engineering in Surveying, Mapping and Remote Sensing, Wuhan University, 2. Chinese Antarctic Center of Surveying and Mapping, Wuhan University

The in-situ exploration of lunar farside is still an international blank until now. The reason is the synchronous rotation of the moon, which results in the unachievable between the lunar farside lander and earth tracking station. The traditional direct tracking mode, such as two-way range/range rate, VLBI delay/delay rate, will be ineffective for the farside lander tracking, therefore it is essential to relay the signal using a relay satellite. In this paper, we firstly give the updated mathematical formulas and the partials for the Four-way Lunar-Orbiter relay tracking measurement. Then, based on the independent precise orbit determination software system WUDOGS, the precise positioning of the lunar farside lander is studied with simulated tracking data. The results show that: with 0.1 mm/s measurement level, the positioning precision of the farside lander could reach the maximum of centimeter level using a circumlunar relay satellite (Fig. 1a); while for the L2 halo relay satellite (Fig. 1b), its accuracy could reach about 10 meters level. The conclusion could provide an important reference for the future lunar farside landing mission, especially for Chinese lunar exploration mission Chang’E-4.

Keywords: lunar farside, lander positioning, precise orbit determination, four-way relay tracking, Chang’E-4

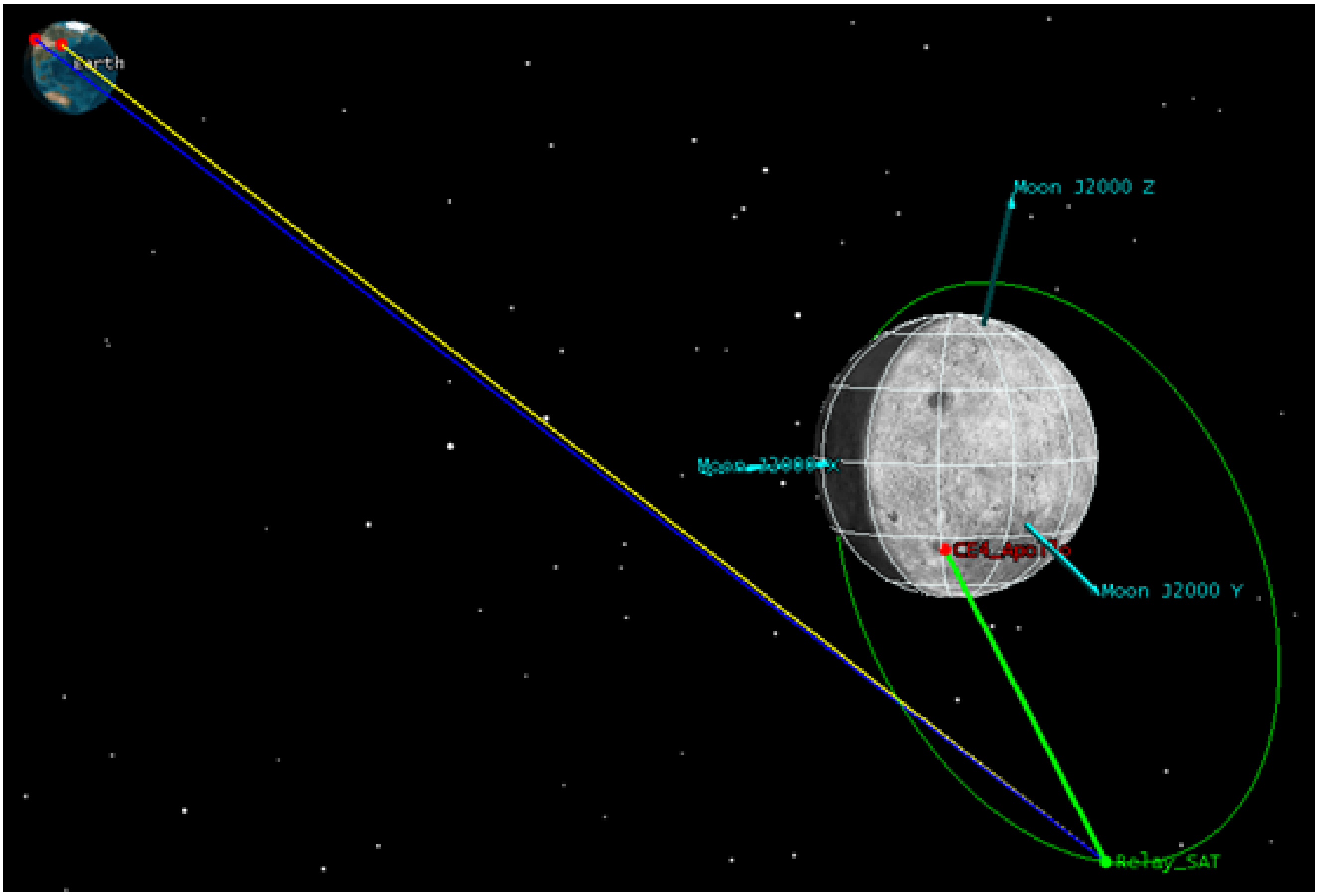
Earth
Moon J2000 Z
Moon J2000 Y
Relay_SAT

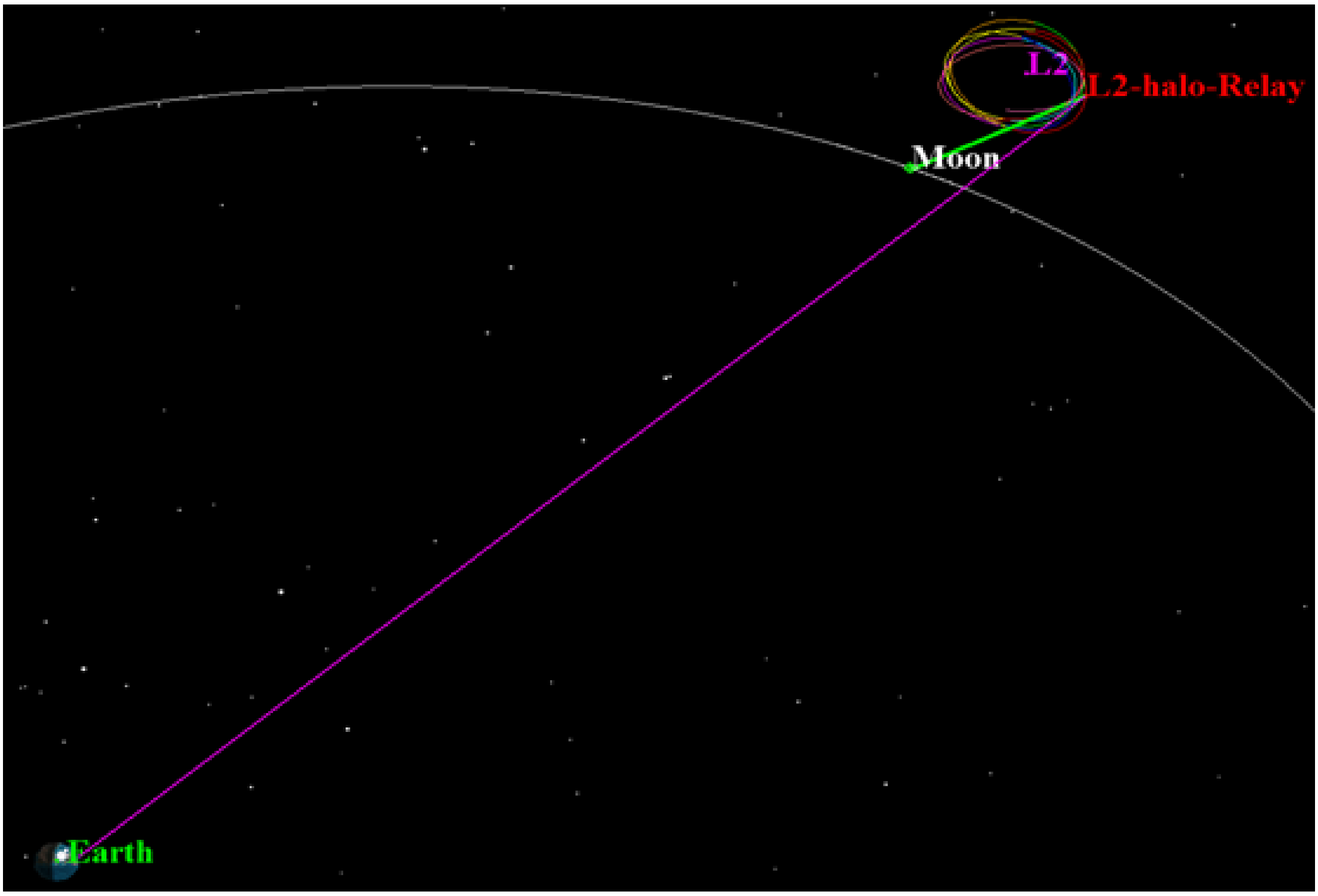
L2
L2-halo-Relay
Moon
Earth

Design and development of Multi-band Camera proposed for SLIM mission

*Kazuto Saiki[1], Hiroaki Shiraishi[2], Chikatoshi Honda[3], Makiko Ohtake[2], SLIM MBC team

1. Graduate School of Science, Osaka University, 2. Japan Aerospace Exploration Agency, Institute of Space and Astronautical Science, 3. The University of Aizu

Smart Lander for Investigating Moon (SLIM) is being planned by Japan Aerospace Exploration Agency (JAXA). SLIM aims to research and demonstrate the engineering key issues related to the smart landing on the gravitational planets. They are precise guidance algorithm, vision based navigation, smart landing gear. By doing SLIM mission, we expect to achieve the paradigm shift in the field of celestial body landing from ‘landing where easy to land’ to ‘landing where desire to land’. This paradigm shift requires a number of novel technologies, and it is reasonable to demonstrate with the small lander at first. We proposed Multi-Band Camera (MBC) for SLIM lander. MBC is a compact VIS-NIR camera composed of an imaging sensor (InGaAs), a filter-wheel with 10 band-pass filters, and a movable mirror for panning and tilting. Scientific objectives of MBC are rock-forming mineral identification and rock texture observation for rocks around the lander. The design of MBC, the state of development, and the idea of scientific operation will be presented.

Keywords: the moon, SLIM, remote sensing

SSERVI: Merging Science and Human Exploration

*Gregory Schmidt[1], Kristina Gibbs[1]

1. NASA Solar System Exploration Research Virtual Institute

NASA's Solar System Exploration Research Virtual Institute (SSERVI) represents a close collaboration between science, technology and exploration, and was created to enable a deeper understanding of the Moon and other airless bodies. SSERVI is supported jointly by NASA’s Science Mission Directorate and Human Exploration and Operations Mission Directorate. The institute currently focuses on the scientific aspects of exploration as they pertain to the Moon, Near Earth Asteroids (NEAs) and the moons of Mars, but the institute goals may expand, depending on NASA's needs, in the future. The nine initial teams, selected in late 2013 and funded from 2014-2019, have expertise across the broad spectrum of lunar, NEA, and Martian moon sciences. Their research includes various aspects of the surface, interior, exosphere, near-space environments, and dynamics of these bodies.

NASA anticipates additional team selections in early 2017 with a further Cooperative Agreement Notice (CAN) likely to be released in 2017. Calls for proposals are issued every 2-3 years to allow overlap between generations of institute teams, but the intent for each team is to provide a stable base of funding for a five-year period. SSERVI's mission includes acting as a bridge between several groups, joining together researchers from: 1) scientific and exploration communities, 2) multiple disciplines across a wide range of planetary sciences, and 3) domestic and international communities and partnerships.

The SSERVI central office is located at NASA Ames Research Center in Mountain View, CA. The administrative staff at the central office forms the organizational hub for the domestic and international teams and enables the virtual collaborative environment. Interactions with geographically dispersed teams across the U.S., and global partners, occur easily and frequently in a collaborative virtual environment. This talk will consist of an overview of SSERVI’s mission and the current US teams.

Keywords: Solar System, Virtual Institute, Lunar, NEA, Martian Moons

NASA’S SOLAR SYSTEM EXPLORATION RESEARCH VIRTUAL INSTITUTE: BUILDING COLLABORATION THROUGH INTERNATIONAL PARTNERSHIPS

*Kristina Gibbs[1], Gregory Schmidt[1]

1. NASA Solar System Exploration Research Virtual Institute

Abstract
The NASA Solar System Exploration Research Virtual Institute (SSERVI) is a virtual institute focused on research at the intersection of science and exploration, training the next generation of lunar scientists, and community development. As part of the SSERVI mission, we act as a hub for opportunities that engage the larger scientific and exploration communities in order to form new interdisciplinary, research-focused collaborations.
This talk will describe the international partner research efforts and how we are engaging the international science and exploration communities through workshops, conferences, online seminars and classes, student exchange programs and internships.

Introduction
NASA’s Solar System Exploration Research Virtual Institute (SSERVI) represents a close collaboration between science, technology and exploration that will enable deeper understanding of the Moon and other airless bodies as we move further out of low-Earth orbit. The Institute is centered on the scientific aspects of exploration as they pertain to the Moon, Near Earth Asteroids (NEAs) and the moons of Mars. The Institute focuses on interdisciplinary, exploration-related science centered around all airless bodies targeted as potential human destinations. Areas of study reported here will represent the broad spectrum of lunar, NEA, and Martian moon sciences encompassing investigations of the surface, interior, exosphere, and near-space environments as well as science uniquely enabled from these bodies.
We will provide a detailed look at research being conducted by our ten international partners. In addition, we will discuss the process for developing internatioal parterships with NASA.

Summary and Conclusions
As the Institute’s teams continue their proposed research, new opportunities for both domestic and international partnerships are being generated that are producing exciting new results and generating new ideas for scientific and exploration endeavors. SSERVI enhances the widening knowledgebase of planetary research by acting as a bridge between several different groups and bringing together researchers from: 1) scientific and exploration communities, 2) multiple disciplines across the full range of planetary sciences, and 3) domestic and international communities and partnerships.

Acknowledgements
The authors would like to thank the hard work and dedication of all SSERVI Team members and International partners that work diligently to create an innovative and collaborative Institute.

Keywords: NASA International Partnerships, SSERVI, Virtual Institute

Comparative Study of the Moon and Mercury: Rupes, their Topography and Origin

*Manabu Kato[1], Hisashi Ootake[1]

1. Institute of Space and Astronautical Science, Japan Aerospace Exploration Agency

Rupes of the Moon and Mercury are comparatively studied on their topography and origin. Images of rupes taken by Kaguya TC and MI, Lunar Reconnaissance Orbiter LROC for the Moon , and MESSENGER MDIS for Mercury are downloaded from Kaguya Data Archives and NASA Planetary Data System. The images are processed and mosaicked to investigate their feature and topography using USGS Integrated Software for Imagers and Spectrometers ISIS program package.
Thirty-one rupes on Mercury are described in IAU approved Gazetteer of Planetary Nomenclature. Only eight rupes of the Moon are named in the list. Rupes are characteristic and remarkable feature in Mercury surface thought to be originated when Mercury's interior cooled and the entire planet shrank slightly as a result. Most rupes in the Moon distribute in the outer edge of mares to attribute their origin to magma eruption. The rupes have never been found in lunar highland and farside except for Rupes Altai in nearside highland.
High resolution images and topographic data of rupes will be referred to show the difference of feature, topography, and origin in the Moon and Mercury.

Keywords: Kaguya, LRO, MESSENGER, rupes, ISIS, mosaics

Extension of the lunar Web-GIS “GEKKO”: Toward statistical analyses of the lunar spectral data

*Shota Iimura[1], Yoshiko Ogawa[1], Yohei Hayashi, Naru Hirata[1], Hirohide Demura[1], Tsuneo Matsunaga[3], Satoru Yamamoto[3], Yasuhiro Yokota, Makiko Ohtake[2]

1. University of Aizu, 2. Japan Aerospace eXploration Agency, 3. National Institute for Environmental Study

The Spectral Profiler (SP) is one of the 14 kinds of observation equipments onboard the Japanese lunar orbiter Kaguya. The spectra of lunar minerals generally have characteristic absorption bands in the observed wavelengths by the SP. By comparing the observed SP spectra with the absorption bands of the known minerals measured in laboratories, we can identify the minerals distributed at the observation spots on the Moon.

A lunar Web-GIS named GEKKO [Hayashi et al, 2016] (Moonlight in Japanese) is a visualization system for the SP data. The GEKKO displays SP observation footprints on the overall images of the Moon on the GIS screen. The users can view the SP spectra observed at the exact spots and download the data very easily just by clicking in the GEKKO system.

Sugimoto et al. [2014] focused on developing a framework for implementing analysis functions to the GEKKO. A few limited functions were implemented for the simplest and preliminary analyses in their study which are not so practical though.

The goal of this study is to extend the framework of Sugimoto et al. [2014] for further implementation of practical analysis functions in the GEKKO. We aim to implement new analysis functions practically used for the VIS-NIR spectral analysis and statistical data analysis. We prepared the extended new framework and succeed in implementing the functions of principal component analysis (PCA) and clustering analysis. Both analysis methods are very major in multivariable data analysis. They are useful for the spectral analyses to understand the distribution of the lunar minerals based on the globally observed data.

In the new framework, the analysis programs are modularized. So the provider can quickly and easily implement various kinds of analysis functions according to the users’ requests. Once such analysis functions are installed, selection or combination out of various kinds of analysis functions are very flexible and completely up to the users. The users see the analysis results quickly on the web site and can get back to check the original SP spectra very easily, too.

The analysis of SP data is essential for the mineral mapping of the Moon. The new framework and implementation of various kinds of analysis functions to the GEKKO is an important step for statistical analyses of the lunar spectral data toward global mapping of the mineral distribution.

.

References:

Hayashi, Y., Ogawa, Y., Hirata, N., Terazono, J., Demura, H., Matsunaga, T., Ohtake, M., Otake, H., "GEKKO" for Hyperspectral Data Distribution: A New Method for Utilizing the Advantages of a Web Map Service, 47th Lunar and Planetary Science Conference, LPI Contribution No. 1903, p.1920, 2016.

Sugimoto, K., Hayashi, Y., Ogawa, Y., Hirata, N., Terazono, J., Demura, H., Matsunaga, T. Yamamoto, S., Yokota, Y., Ohtake, M. Ootake, H., Development of a web application for dynamic analysis of the Kaguya Spectral Profiler data, Japan Geoscience Union Meeting 2014, Pacifico Yokohama, Japan, May 2014.

Keywords: GEKKO, Spectral Profiler, Kaguya, Geographic Information system , Principal Component Analysis, Cluster Analysis

Implementation of assortment algorithm for excluding noisy data in the lunar web-GIS: GEKKO

*Yuya Matsubara[1], Yoshiko Ogawa[1], Makiko Ohtake[2], Yohei Hayashi, Naru Hirata[1], Hirohide Demura[1], Tsuneo Matsunaga[3], Satoru Yamamoto[3]

1. University of Aizu, 2. Japan Aerospace eXploration Agency, 3. National Institute for Environmental Study

The lunar web-GIS “GEKKO” [Hayashi et al., 2016] is a very convenient system for the users to view the observed spectra on the Moon with the surface images. The main objective of developing the GEKKO is to display the Spectral Profiler (SP) data and visualize the information of the minerals brought out from the data. The SP is a spectrometer, onboard Kaguya which is a Japanese lunar orbiter. The SP observed the visible-near infrared reflected spectra of the lunar surface right under the satellite. We can identify the minerals and constrain the minerals the distribution on the Moon by detecting the absorption bands of the observed spectra. The web-GIS “GEKKO” plots observation footprints of SP on the lunar surface image. When users select any observation point, the GEKKO displays the graph of the SP spectra observed at the spot, the table to show ancillary data, and the high resolution image taken by imager, onboard Kaguya. The users can also download SP data very easily through this GEKKO system too. SP data analysis functions are also implemented in the GEKKO system recently. The analysis system has been installed by Sugimoto et al. [2014] and Iimura et al. [2017]. Sugimoto et al. [2014] developed a framework for real-time analysis of SP and implemented very simple functions of similarity analysis. Iimura et al. [2017] extended the framework of Sugimoto et al. [2014] and implemented practical functions:- principal component analysis (PCA) and clustering analysis. The current GEKKO is useful for viewing and analyzing SP data, however, the system uses and displays all the SP data amounting to about 70 million spectra which include noisy data. The S/N ratios of SP data depend on observation conditions. The noisy data should not be used for the analysis without caution. Especially, in statistical analysis such as PCA using a bunch of data, stacking of noise could affect the results critically and prevent with appropriate evaluation and understandings. Thus, this study tries to evaluate the noise first and develop the algorithm to classify the low-quality SP data. We developed and implemented the new function to discriminate low-quality data in the GEKKO. When users use this function, the data judged as of low-quality are shown by changing the colors of SP footprints where such noisy data are observed. The judgement criteria can be chosen by users flexibly. The users can also tune and adjust the controlling parameters for discriminating noisy data. Thereby, users can check quality of each SP data and select SP data with the higher S/N ratios according to user's objectives or preferences.

Keywords: moon, Kaguya(SELENE), Spectral Profiler, web-GIS, GEKKO, noise evaluation

Improvement of the extraction method of lunar secondary crater using the Voronoi tessellation

*Yuhi Yasuda[1], Chikatoshi Honda[1]

1. The University of Aizu

One of the estimation methods of formation age of planet surface is the crater chronology. Generally, craters are increasingly formed on the planet surface at random over time. From this perspective, the crater chronology utilizes the crater number density to estimate the formation age of planet surface. When we utilize the crater chronology, we should exclude secondary craters. Secondary craters are formed by ejecta thrown out from primary crater produced by the impact object from interplanetary space. The characteristic of secondary craters shape is clustered or chained with herringbone patterns. Thus, if we could not discriminate between primary and secondary craters, it causes an error of the estimation formation age. Although Kinoshita (2014) extracted lunar secondary craters based on the Voronoi tessellation of craters, some secondary craters were not extracted. Therefore, I tried to further develop the algorithm based on Kinoshita (2014) to extract such secondary craters and decrease the error between the result of my improvement method and the result of visual inspection. As a result of my improvement, the error between the result of my improvement method and the result of visual inspection is decreased by 15% compared with the method based on Kinoshita (2014).

Keywords: moon, secondary crater, the Voronoi tessellation

Positive openness map for visual inspection of fault scarp associated with lunar wrinkle ridges

*Tomokazu Sato[1], Chikatoshi Honda[1]

1. University of Aizu

Wrinkle ridges are topographic features observed often in plains of the moon. Both edges of wrinkle ridge have scarps related to the fault slip in the subsurface. According to a hypothesis of the origin of wrinkle ridges (e.g., Suppe et al., 1983), the scarps are defined as fore-limb and back-limb, and the fore-limb which has abrupt slope compared with back-limb corresponds to a fault scarp. These fault scarps are formed by horizontal pressure related to tectonic deformation of subsurface of the moon. The spatial distribution and their scale of fault scarps with wrinkle ridges lead us to understand the evolution of the lunar subsurface.
We applied the positive openness as a representative parameter of solid of the sky extent over a point of interest as a parameter for preparing effective data to identify candidates of fault scarps associated with wrinkle ridges. Positive openness map could be calculated from lunar Digital Terrain Model (DTM) acquired by Terrain Camera/Kaguya. Radial limit which is the range of positive openness calculation for the interest, affects the difference in vision of enhancement of topographic features. As a result of several radial limits calculations, we adopted radial limit of 222 m as a most appropriate one. By using of positive openness map, we could found several candidates of fault scarps associated with wrinkle ridges.

Keywords: moon, wrinkle ridge, positive openness map

Automatic detection of lunar sub-km craters via deep learning

*Riho Ito[1], Ryosuke Nakamura[1], Chikatoshi Honda[2]

1. National Institute of Advanced Industrial Science and Technology, 2. The University of Aizu

Crater chronology is a method that estimates generated age on surface of a body from size-frequency distribution (SFD) of impact craters. Coordinates and diameter are needed for computing SFD, and measurement accuracy of crater information is factored into the estimation accuracy of crater chronology. So, highly accurate crater information is important for discussing evolution process of the lunar surface. We can sufficiently detect smaller than 1km craters because spatial resolution of lunar observation data is improved, for example, resolution of Terrain Camera (TC) ortho data is 7.4m/pixel to 10.0m/pixel. TC ortho data were generated by SELENE observation data. However, manually detecting sub-km crater take an immense amount of time because number of crater is increase exponentially with decreasing crater diameter. For solving these tasks, automatically crater detection algorithms (CDAs) have been studied. Goal of these studies is to generate high accuracy crater information enough to apply crater chronology. For detecting martian craters from high resolution (12.5m/pixel) panchromatic imagery that was captured by High Resolution Science Camera aboard Mars Express spacecraft, Joseph et al. (2016) proposed a CDA with Convolutional Neural Network (CNN). CNN is part of deep learning methods. By designing the neural network architecture that has more multi layers, deep learning can represent the data more abstract. From supervised data, deep learning can learn optimal features that are needed for feature extraction process and data identification process. Especially, CNN keeps high performance in the field of computer vision (for example, image recognition, sound recognition). Joseph et al., (2016) reported that results of crater detection by using CNN get more high performance than other CDAs (Bandeira et al., 2010; Urbach and Stepinski, 2008).

Purpose of this research is to entertain sub-km CDA by using CNN with TC ortho imagery. By using high resolution imagery, to be able to detect smaller craters than before will be expected. A part of important things for deep learning is to prepare many supervised data. In this research, by detecting craters in manually, we prepared a crater dataset that includes 185 m to 1 km in diameter craters on Mare Imbrium(footprint of a TC ortho image: TCO_MAPm04_N24E333N21E336SC). The TC ortho image was divided into 3 regions (north, center and south). The crater datasets was detected by manually. The center region and the south region were used for learning, and the north region was used for evaluation. Input data for CNN were small patches that were cropped based on each crater diameter, and all patches were scaled 15 x 15 pixel. Positive sample is that craters are included, and negative sample is that craters are not included. In fact, CNN learned classifier task that "are there craters in a patch or not?" In this result, patch based classification accuracy was over 90 %. Additionally, we tried image based classification (crater detection from a part of north area image). In this result, CNN could detect position of craters, but could not detect shape and there were many false detections about object that has similar features to craters.

Keywords: Deep Learning, Crater Detection

Influence on illumination condition by analysis altitudes

*Inoue Hiroka[1], Hisashi Otake[1], Makiko Ohtake[1], Mitsuo Yamamoto[1], Takeshi Hoshino[1], Takanobu Shimada[1], Satoshi Tanaka[1], Koichi Masuda[1], Hitoshi Morimoto[1], Sachiko Wakabayashi [1], Tatsuaki Hashimoto[1]

1. Japan Aerospace Exploration Agency

The Japan Aerospace Exploration Agency (JAXA) launched a Moon orbiter, Kaguya, in September 2007 and succeeded in putting it into an orbit approximately 100 kilometers above the Moon in October. This Moon orbiter has provided us with a significant amount of scientifically valuable Lunar data. Besides Japan, various other countries all over the world have succeeded in obtaining Lunar observation data using Moon orbiters such as NASA’ s Lunar Reconnaissance Orbiter (LRO). The future objective of Moon exploration is to investigate the existence of volatiles such as water and sodium, and to search their potential usefulness. Since valuable resources are likely to exist in the lunar polar region, some countries are currently planning landing missions around the lunar poles. JAXA is also considering a Moon polar exploration mission whose purposes are to investigate the existence of lunar resources and to study their potential. For such a mission, we must select a landing site with long-term desirable sunlight conditions because the mission period is expected to be long due to the observation at the site. Illumination condition analysis of the south pole has been well studied, but that of the north pole is insufficient even though a superiority of the south pole for a landing site has not fully examined. Landing site selection is critical for the mission accomplishment in the polar region, so much previous work has well analyzed illumination conditions in the Moon polar region. The Moon has more undulating terrain than the Earth, so sunshine conditions change remarkably with the altitude or sunshade. Hence, we determine an appropriate landing site and calculate the illumination conditions for the landing site assuming three different altitudes.

We employed Digital Elevation Model (DEM) data obtained by the Lunar Orbiter Laser Altimeter (LOLA) of LRO and the Terrain Camera (TC) of Kaguya. In addition, we used the SPICE toolkit to calculate the position of the Sun. By combining the DEM data and Sun position, we can calculate the ratio of solar disc occulted by the horizon. We first conducted the simulation of illumination condition over a 60 km square around the lunar north pole. Within the good illumination condition area, there are especially favorable sites that satisfy the conditions for landing that the surrounding area also has good sunshine and smaller differences in height. For the candidate landing sites, we did not regard the Sun as one light source but separated it into 52 sun discs, and simulated illumination for altitudes of 0, 2, and 5 meters.Figure represents changes of sun visibility with each altitude. The colorbar shows the number of sunshine days in two years.

We present the illumination simulation results of an especially favorable landing site using LRO and Kaguya data. We can obtain the detailed sunshine conditions or its difference with altitude by conducting simulation with changing altitude. Future work will focus on the illumination simulation for a wider range of regions for precise landing site selection. In addition, we must evaluate the influence of resolution of input DEM data on illumination conditions.

Keywords: Moon, Analysis of illumination conditions, Polar region

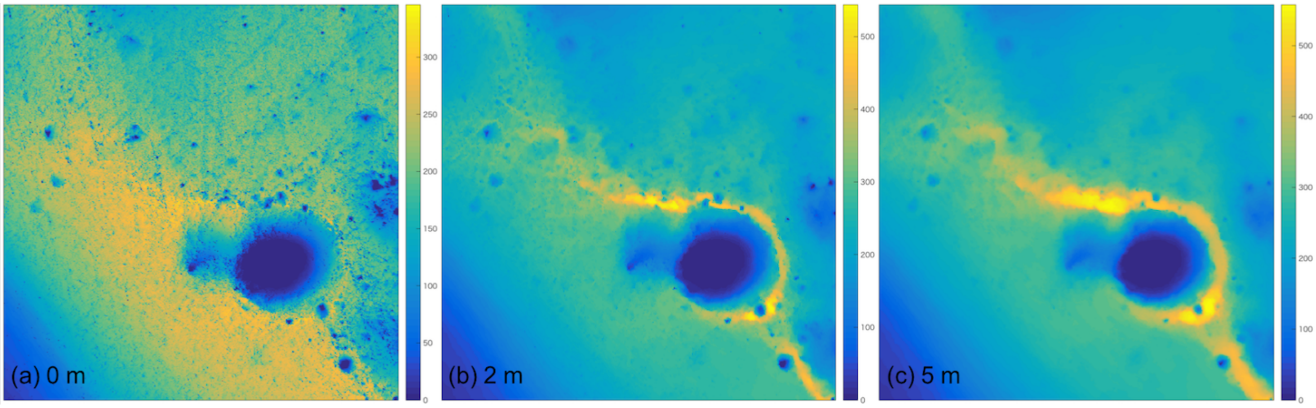
(a) 0 m
(b) 2 m
(c) 5 m

Geological map of Mare Smythii based on the SELENE observation data

*Ken Ishiyama[1]

1. Institute of Space and Astronautical Science, Japan Aerospace Exploration Agency

Lunar geological map is useful for understanding the process of lunar tectonics and volcanic activity, so the high-resolution terrain and spectral cameras has updated the lunar geological map day by day [e.g., Brennan, 1975; Hiesinger et al., 2010]. Thus, these surface information produced the present lunar geological map, but on which, the subsurface information was not reflected. This information gives the subsurface structure, its stratigraphy, and the thickness of subsurface lava flow layer, so becomes important clue of lunar tectonics and volcanic activity.
In this study, I focused on Mare Smythii, which is located at 2°S, 87°E on the Moon. The surface of Mare Smythii is covered only by one lava flow, which erupted ~3.14 Ga ago [Hiesinger et al., 2010]. According to the SELENE/Lunar Radar Sounder observation, the several subsurface boundaries were founded in Mare Smythii [Ono et al., 2009; Kobayashi et al., 2014]. The part of subsurface boundary outcropped on Mare Smythii, so we concluded that the surface of Mare Smythii was composed of two lava flows at least; the subsurface information succeeded in updating the geological map of Mare Smythii. In the presentation, I will report the preliminary geological map of Mare Smythii.

Distribution of Olivine and Plagioclase around the Crisium Basin on the Moon

*Yuji Agatsuma[1], Naru Hirata[1]

1. The University of Aizu

Global distribution of purest anorthosite (PAN) and olivine on the Moon has been revealed (Ohtake et al., 2009, Yamamoto et al., 2010, 2012), but mineral distribution on certain local regions have not often been discussed. Detailed analysis on local regions is also important to examine the lunar crustal structure. Sugamiya and Hirata (2015) revealed distribution of olivine, plagioclase and pyroxene in the southwest rim of the Crisium basin where the existence of these minerals were previously reported (Yamamoto et al., 2010, 2012). They used Multiband Imager (MI) data onboard SELENE (Kaguya). MI has high spatial resolution and it enables us to examine the whole region of the moon without gap. In this study, we expand the target region of their work to whole sector by investigating distribution of olivine and plagioclase around the Crisium basin using same method as Sugamiya and Hirata (2015). We found a wide and homogeneous distribution of olivine and plagioclase around the Crisium basin. As Sugamiya and Hirata (2015) have already been stated, sites of these minerals are associated to small craters around the basin. We found that the CSFD for craters associating olivine site almost matches the isochron for 3.44 Ga, expected age of the Crisium basin, in the size range of over 6 km in diamter. This means that olivine can be detected in almost all craters larger than 6 km in diameter, and olivine is commonly distributed in the ejecta of the Crisium basin beneath over 600 m from the surface.

Keywords: Lunar crust, olivine, plagioclase, Multiband Imager

Study on lunar Mg, Fe and carbon-bearing rocks formed at extreme condition

*Yasunori Miura[1]

1. Visiting (Yamaguchi, AIC University)

The Moon has been discussed as to whether it has evolved from water-Earth or is an unique Earth planet compared to air-planets of Mars and Venus, or water-planet Earth. Author studied in present study is based on recent model that the Moon produces local gas and fluids remained on surface basaltic rocks with carbon-volatiles but without global active system, which is main purpose of the present paper as follows.

1. Solid rocks in any celestial bodies (including the Moon basically) have been accumulated from nano-particle to macro-grains by evaporating volatile-elements as buffer roles above the solidified rocks.
2. There are three types of global systems in the Earth-type planets. The solid rock system is remained globally by various collision phenomena, but generation of local gas or liquid states above the rock. Mars and Venus have global air-system, and our Earth has global air- and water-systems above the solid rock as different planets.
3. Carbon-bearing solidified grains exist in fine scale widely during the three-state changes of celestial bodies development. The carbon can be remained during extreme condition by exchanged states state, which suggests that the elemental abundance of carbon element is richer in quenched carbonaceous chondritic meteorite than the crust rocks of Earth clearly. The carbon-bearing solid grains is considered to be an "extreme-condition (shocked) indicator" showing active state change.
4. Lunar basaltic rocks show high Mg, Fe and carbon contents in the Apollo lunar and meteorite samples. The basalts are therefore volcanic rocks solidified on the surface in the extreme state of meteoritic impacts on the primordial periods of the Moon. Basaltic compositions formed by extreme condition are difficult to be distinguished from the surface shallow or deep interior of mantle origins at the present evolved today. The carbon element mixed in the solidified grains during basaltic formation can be found as high pressure-type carbons (as diamond sources) now, where volatile carbon can be found even in deep interior today. Quenched rock containing carbon-bearing fine grains can be observed by nanotechnology with an high-sensitive electron microscopy, which will be shown in author’s presentation in the plenary session of the JpGu-AGU 2017.

The present study can be summarized as follows. 1. The basaltic rocks on the lunar surface can be pointed out from the bulk compositional characteristics formed in the extreme impact condition. 2. Fe, Mg and carbon are remained in the rock surface of the shocked glassy solids. 3. Carbon-bearing fine grains called here as "extreme-condition (shocked impact) indicator" can be observed on the solidified surface rocks. 3. Igneous rocks formed by the impact process are widely formed on the shallow surface of a celestial body to deep interior during its evolution process finally, which can be also applied to the igneous rocks contained carbon volatiles in the mantle rocks globally. 4. The present results of primordial basaltic rocks with carbon remnants indicate that there is no global fluid ocean water-Earth system in the Moon and other planets relatively.

Keywords: Carbon-bearing grains, The Moon, Basalt

U-Pb systematics of lunar meteorite NWA 2977

*Narumi Moromoto[1], Kentaro Terada[1], Yosuke Kawai[1], Masaaki Miyahara[2], Yuji Sano[3], Naoto Takahata[3]

1. Osaka University Graduate School of Science, 2. Hiroshima University Graduate School of Science, 3. Atmosphere and Ocean Research Institute, The University of Tokyo

The lunar meteorites are important because they would give us a new insight into the unexplored region of the Moon. North West Africa (NWA) 2977 is identified as olivine cumulate lunar meteorite, which was discovered in Morocco in 2005. So far, we have found a remarkable shock melt vein (SMV) in the thin section, which had suffered from the impact melting and rapid cooling.
In this study, in order to investigate the thermal history of NWA 2977, we carried out the in-situ U-Pb dating of phosphate grains in/out of the SMV, using Nanoscale Secondary Ion Mass Spectrometer (NanoSIMS) at the Atmosphere and Ocean Research Institute, University of Tokyo. Most of the phosphates give a crystallization age of 3132±67 Ma (1 σ). Whereas, one grain out of the SMV shows a slightly disturbed U-Pb systematics, indicating the very recent shock event (< 346 Ma). At the conference, we also discuss μ-value ($^{238}U/^{204}Pb$) of NWA2977.

Role of volatiles during late-stage crystallization of intercumulus pockets: Comparison of the NWA 773 clan of lunar meteorites with terrestrial gabbro from Murotomisaki, Japan

*Timothy Fagan[1], Jun Uchida[1], Takatsugu Asahi[1]

1. Department of Earth Sciences, School of Education, Waseda University

Introduction: Late-stage intercumulus pockets in the olivine cumulate (OC) lithology of the Northwest Africa 773 clan of lunar meteorites are enriched in incompatible elements [1]. Pyroxene crystals adjacent to the pockets are zoned, with Ti# (Ti/[Ti+Cr]) increasing and Fe# (Fe/[Fe+Mg]) remaining constant as the pockets are approached, providing an example of igneous differentiation on the Moon [1]. The pockets are also of interest because they typically contain the Ca-phosphates merrillite and apatite; apatite crystals in the pockets contain F, Cl and OH in various ratios, reflecting the composition and abundance of volatile elements during late-stage crystallization of the OC [2-4]. The presence of H_2O in the apatite indicates that water was present in pockets of residual liquid trapped in the OC; however, the abundance of water and effect of water on late-stage crystallization have not been resolved.

In this study, we (1) compare late-stage pockets of NWA 773 clan OC with pockets in terrestrial gabbro from a sill in Murotomisaki, Japan [5], and (2) determine F:Cl:OH ratios in lunar apatite using low-voltage EPMA (electron probe micro-analysis; see below). The main goals are to evaluate and compare the roles of volatiles, particularly water, during late-stage crystallization in lunar and terrestrial gabbros.

Methods: We compared minerals and textures of late-stage pockets from the Murotomisaki sill with pockets from NWA 2977 and NWA 773. In this study, our main observations are based on one sample (Muro-14) collected from the coarse gabbro unit in the central part of the sill [5]. We compared Muro-14 with a polished thin section (pts) of NWA 2977, which is part of the NWA 773 clan and consists entirely of OC [6,7]. Images of minerals and textures were collected using petrographic microscopes, SEM (BSE images, Hitachi S-3400N) and EPMA (BSE and x-ray elemental maps, JEOL JXA-8900). Major element compositions in feldspar were collected by EDS using the SEM and by WDS using the EPMA. Changes in feldspar composition were compared to distance from pockets.

Determining the ratios of F, Cl and OH in apatite is difficult because F and Cl K-alpha X-rays typically vary during exposure to an electron beam [8] and OH cannot be detected by EPMA. So, we have been developing an EPMA technique (in collaboration with D. Harlov; see [9]) that uses low voltage (7 kV) to limit variations in F and Cl count rates. A small spot size (~ 1 μm) is desired because of the small grain size of much apatite in NWA 773.

Results: In both Muro-14 and NWA 2977, plagioclase is zoned, with more Ab-rich compositions closer to the pockets. In NWA 2977, feldspar varies from Ab_{05} to Ab_{15}, whereas the Muro-14 feldspar is much more albitic (Ab_{40} to Ab_{95}). Discontinuities in zoning and porosity in feldspar closest to the Muro-14 pockets suggest that H_2O-rich fluid from the pockets interacted with feldspar, resulting in albitization. Some discontinuities also occur in NWA 2977, but it is not known if feldspars adjacent to pockets in NWA 2977 interacted with a volatile-rich fluid.

Most analyses of apatite in NWA 773 are F-rich, but variations in F/Cl at low OH and F/OH at low Cl occur in different petrologic settings. Data from [2] combined with our results show that NWA 773 OC pockets vary in F/OH at low Cl, suggesting some enrichment in H_2O during late-stage formation of the pockets.

References: [1] Fagan T.J. et al (2014) GCA 133: 97-127. [2] Tartese R. et al (2014) MaPS 49: 2266-2289. [3] Boyce J.W. (2014) Science 344: 400-402. [4] Asahi T. (2016) Goldschmidt Conference Abstracts 115. [5] Hoshide T. et al (2006) J. Min. Pet. Sci. 101: 223-239. [6] Zhang A-C. et al (2011) MaPS 45:

1929-1947. [7] Nagaoka H. et al. (2015) Earth Planets Space 67: 200, 1-8. [8] Stormer J.C. et al (1993) Am. Min. 78: 641-648. [9] Schettler G. et al (2011) Am. Min. 96: 138-152.

Keywords: gabbro, volatile elements, water

Performance of the pyroelectric X-ray generator developed for active X-ray spectrometer on future lunar and planetary landing missions

*Hiroshi Nagaoka[1], Nobuyuki Hasebe[1,2], Masayuki Naito[2], Miho Mizone[2], Haruyoshi Kuno[1]

1. Research Institute for Science and Engineering, Waseda University, 2. School of Advanced Science and Engineering, Waseda University

Planetary landing missions to the Moon and Mars have been recently performed. In Japan, future lunar landing mission have been also planned. The landing missions investigate the geology at landing site in detail. One of powerful methods to determine the elemental composition of the planetary surface is X-ray fluorescence spectrometry. We have developed active X-ray spectrometer (AXS) in order to apply the AXS for future lunar landing mission as elemental analyzer. The AXS consists of pyroelectric X-ray generators (PXG), and a silicon drift detector (SDD). Laboratory experiments have been conducted to obtain enough X-ray intensity from PXG to measure the major and important elements as Mg, Al, Si, K, Ca, Ti and Fe in short observation interval. Furthermore, we have developed a prototype of PXG with a high intensity of X-ray. In this work, the development and performance of present PXG will be reported and discussed.

Keywords: XRF, element

INTERNAL STRUCTURE OF THE MOON INFERRED FROM APOLLO SEISMIC DATA, SELENODETIC GRAIL AND LLR DATA AND THERMODYNAMIC CONSTRAINTS

Ekaterina Kronrod[1], *Koji Matsumoto[2], Ryuhei Yamada[3], Oleg Kuskov[1], Victor Kronrod[1]

1. Vernadsky Institute of Geochemistry and Analytical Chemistry (GOKHI RAS), 2. RISE Project, National Astronomical Observatory of Japan, 3. The University of Aizu, Research Center for Advanced Information Science and Technology

In the recent paper (1) lunar interior models by complementing Apollo seismic travel time data with selenodetic data which have recently been improved by GRAIL and LLR. Important information on the thickness of the crust, LVZ, core structure and seismic velocities was obtained. But this problem statement retains lunar mantle composition to be uncertain. In (2,3) mantle composition can be simulated based on thermodynamic approach and petrological evidence from seismic data, MOI and mass. The goal of this paper is to investigate lunar internal structure models which are consistent with the seismic and the selenodetic (GRAIL and LLR) data and thermodynamic constraints.
We apply spherically symmetric viscoelastic hydrostatic model of the Moon (1). The Moon consists of nine layers: megaregolith, crust, four-layers mantle, low viscosity zone (LVZ), liquid outer core and fluid inner core. In each zone physical properties are assumed to be constant. We employed same data as (1): four selenodetically observed data of mean radius, mass, MOI, and tidal Love number *k2* (4). Seismic travel time data was selected by (5).
Geochemical models of bulk Al and Fe composition: Currently there are two main groups of geochemical models of the Moon (6): 1. Moon's composition with Al content similar to models with Earth's Al_2O_3 content; 2. The Moon is enriched in Al against Earth. We consider models with Earth's Al_2O_3 content. Analysis of majority of current Moon's composition models (6) revealed that for group 1 Al_2O_3 = 4,05 ± 0,36 wt.% and Fe_2O_3 = 12,25 ±1,33 wt.%. Division mantle into 4 layers was performed according to (7) model. Concentrations of main oxides were equal in first 3 upper mantle layers (Mantle 1-3 in Fig.1) and we applied the model of magma ocean to calculate oxide concentrations in fourth lower mantle layer (Mantle 4 in Fig.1) (which implies that concentrations of main oxides in the lower mantle is equal to average concentrations in upper mantle and crust and equal to bulk concentrations). The models of the magma ocean in such a formulation were considered in our previous work (3). Temperature in the lunar mantle is defined by equation from (8).
Thermodynamic approach: The general our methodology is to combine the geophysical and geochemical constraints and thermodynamic approach, and to develop, on this joint basis, the self-consistent models of the Moon. The crustal composition of Taylor (1982) are taken as representative of the crust material. Thermodynamic modeling of phase relations and physical properties in the multicomponent mineral system CFMAS was used to develop a method for solving the inverse problem [3].
Inversion: A Bayesian inversion approach is an effective method to solve for a nonlinear problem such as planetary internal structure modeling, e.g., [7], [9]. The solutions of the parameters and their uncertainties are obtained from the posterior distribution which is sampled by the MCMC algorithm. In the present model bulk Al content and bulk Fe content are included into likelihood function (LHF).
Results: The main results are shown in Fig.1. Probable concentration of Al_2O_3 is 2,7-2,9 wt.% in the upper mantle and 4,1-4,3 wt.% in the lower mantle. Bulk Fe_2O_3 is within 11,5-12,5 wt.%. Seismic P-wave velocity (~7,92 km/s) in the lower mantle is close to lower bound of velocity range from (7). From these results it can be concluded that the models of the Moon with Earth's bulk Al content is in a good agreement with geophysical data.

References: [1] Matsumoto et al. (2015),GRL, 42, i18, 7351–7358; [2] Khan et al.(2007), Geophys. J.,168, 243–258; [3] Kronrod, Kuskov (2011) Izvestiya. Phys. Solid Earth (Rus), 47, 711-730; [4] Williams J. G. et al. (2014) *JGR, 119*, 1546- 1578; [5] Lognonne P. et al. (2003) *EPSL, 211*, 27-44; [6] Kuskov O.L.et al. (2014) *PEPI*, 236, 84-95; [7] Gagnepain-Beyneix et al. (2006) PEPI,159,140–166; *[8] E. V. Kronod et al.* (2013), Solar System Study: 4M-S3 IKI RAN,94-104.

Keywords: Moon, internal structure, numerical simulation, thermodynamics, composition

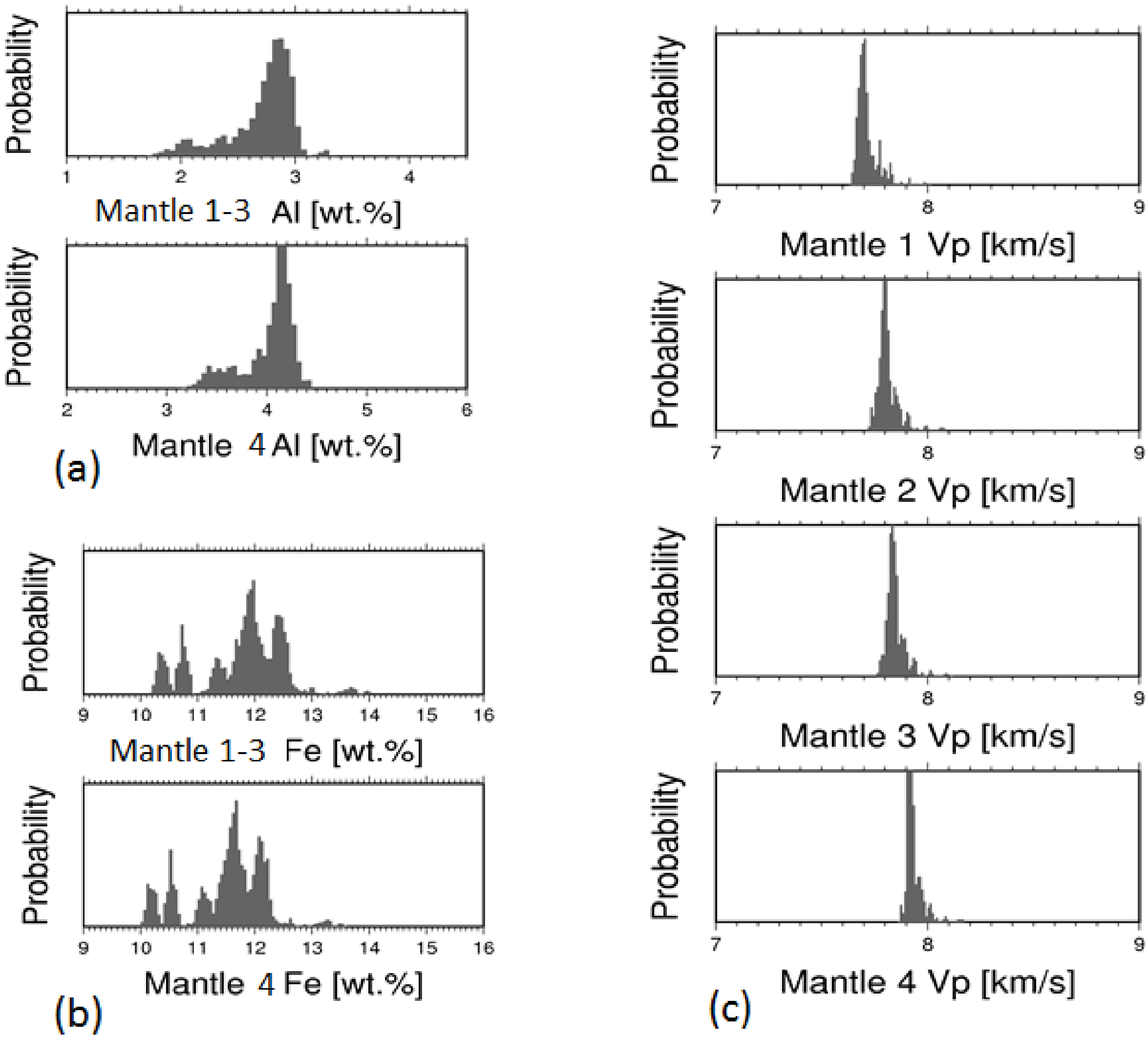

Fig. 1 Posterior probability density functions: Al (a) and Fe (b) concentrations and P-wave seismic velocities distribution in layers 1-4 of the lunar mantle.

NUMERICAL SIMULATION OF LUNAR SURFACE CHARGING AND ELECTROSTATIC DUST LOFTING DUE TO SOLAR WIND AND UV IRRADIATION

*Necmi Cihan Orger[1,2], J. Rodrigo Cordova Alarcon[1,2], Kazuhiro Toyoda[1,2], Mengu Cho[1,2]

1. Kyushu Institute of Technology, 2. Laboratory of Spacecraft Environment Interaction Engineering

The interaction with the surrounding plasma has several effects on the Moon, and one of them is suggested as electrostatic transportation of the lunar dust grains while the lunar surface is simultaneously charged by the continuous flux of the ambient plasma and the solar irradiation. The lunar surface emits photoelectrons when it is exposed to the solar ultraviolet and X-ray radiation, and this photoemission current establishes a current balance with the secondary electron emission and the collection of electrons and ions from incoming plasma. Since the Moon orbits the Earth under the solar wind influence most of the time, the upstream plasma conditions are typically driven by the solar activity. In addition, the lunar surface potential, electric field and Debye length change with variations in solar wind conditions, and the lunar dust grains can be lofted and/or levitated above the surface according to the current sources. Therefore, the conditions of fast and slow stream solar wind as well as post-shock plasma, early CME and late CME passages are investigated in order to figure out how the lunar dust particles can reach higher altitudes in this study. In addition, the electrostatic forces acting on the submicron-sized lunar dust particles are compared to the gravity and cohesive forces. Through the numerical simulations of the lunar surface and dust charging, the following outcomes were obtained. First, it has been observed that solar flare events produce strong electric field on the dayside of the Moon, and the dust grains can travel through dense and thin plasma sheath above the dayside surface. Second, very cold and low-density plasma, which can be seen during early CME passages, creates large positive potentials on the subsolar point similar to the solar flare events. Third, the results showed that strong electrostatic forces are not sufficient solely to loft the dust particles to higher altitudes since the time to travel through the plasma sheath above the surface is important to accelerate the charged dust grains to proper velocities. Lastly, the post-shock plasma limits the positive charging of the subsolar point while it increases the electrostatic force acting on the dust grains above the terminator region.

Keywords: lunar dust, lunar surface charging, dust lofting, solar wind, coronal mass ejection

Science Objectives and Status of the Next Generation Lunar Retroreflector

*Douglas G Currie[1], Giovanni Delle Monache[2], Bradford Behr[1], Simone Dell'Agnello[2]

1. Department of Physics, University of Maryland, College Park, USA, 2. INFN-LNF, Frascati, Italy

The design performance of the Next Generation Retroreflector (NGR), also known as the Lunar Laser Ranging Array Retroreflector for the 21st Century and/or MoonLIGHT depends critically on a detailed thermal analysis to optimize the design. This consists of three phases. The first, which will be the primary focus of this talk, consists of optimizing the performance with respect to the physical parameters of the package, conductivity, emissivity and reflectivity of various elements. This will be the primary focus of this talk, illustrating some initially surprising results. The second consists of optimizing the parameters of the CCR (the back angle offsets) in the presence of phase 1 conclusions. The third phase consists or readdressing the physical parameters of the package at the optimized back angle offsets. Updates on other issues will be briefly addressed: future landing sites and the required of a new design for the NGR,

Current status of the Next Generation Retroreflector (NGR) will be described. This will address the current schedule and future landing sites. In addition, interesting effects that have been recently discovered concerning break-through in solid CCRs, thermal effects in the CCR that affect the return signals, detailed simulations of the effects of atmospheric propagation and a candidate for a low absorption high emissivity coating will be briefly considered.

Keywords: Lunar Laser Ranging, Next Generation Lunar Retroreflector, Thermal Simulation